

Fabrication and Characterization of rGO/Tin Oxide Nanocomposite using Hydrothermal Technique



By

Rizwan Ullah

Reg. No: NUST201260691MSCME67712F

Supervisor

Dr. Amir Habib

**School of Chemical and Materials Engineering (SCME)
National University of Sciences and Technology (NUST), H-12
Islamabad, Pakistan
September, 2015**

Fabrication and Characterization of rGO/Tin Oxide Nanocomposite using Hydrothermal Technique



Name: Rizwan Ullah

Reg. No: NUST201260691MSCME67712F

**This work is submitted as a MS thesis in partial fulfillment of the
requirement for the degree of**

(MS in Materials and Surface Engineering)

Supervisor: Dr. Amir Habib

School of Chemical and Materials Engineering (SCME)

National University of Sciences and Technology (NUST), H-12

Islamabad, Pakistan

September, 2015

Thesis Submission Certificate

It is to certify that work in this thesis has been carried out by **Rizwan Ullah** and completed under my supervision in School of Chemical and Materials Engineering, National University of Science and Technology, H-12, Islamabad, Pakistan.

Supervisor

Dr. Amir Habib

Submitted Through

Principal/Dean

School of Chemical and Materials Engineering

National University of Science and Technology

DEDICATION

To my lovely parents, respectable teachers and dearest friends

ACKNOWLEDGEMENT

*First of all I present my humblest and earnest thanks to Almighty **Allah**, The Most Sympathetic and The Merciful, Who blessed me with power to accomplish this project.*

*I offer my sincerest gratitude to my supervisor, **Dr. Amir Habib**, who has supported me throughout my thesis with patience and knowledge whilst allowing me to work in my own way. I attribute the level of my Master's degree to their encouragement and effort.*

*I would really like to extend my thanks to all the **lab staff** for their assistance, my friends **Mr. Tanveer**, **Mr. M.Umar**, **Mr. Jamshid Ahmad** and **Mr. Shafi-Ur-Rehman** and grateful for their kind, friendly and moral support in my work as well as their company and cooperation during the times when I am encountered with difficulties.*

*In the end, my humble is to my dear parents who always prayed to **Allah** Almighty for my success and brought me with all her efforts. I would also like to pay my special tribute to my **wife** who encourage and supported me during all this period.*

Rizwan Ullah

ABSTRACT

Tin Oxide is an important inorganic semiconductor material because of its unique properties such as electrical conductivity, high optical transparency and sensitivity to chemicals drawn considerable attention due to its broad applications in various fields such as gas sensors, dye sensitized solar cell, field emission and supercapacitors while graphene sheet which is 2D nonmaterial showing high carrier mobility at room temperature have further intensified interest in this material. Graphene sheet decorated with metal oxide nanoparticles can perform multiple roles including photocatalyst, adsorbent, lithium ion batteries (LIBs) and gas sensing characteristics.

This thesis is based on synthesis of rGO/SnO nanocomposite via hydrothermal method with SnCl_2 and graphene oxide (GO) as the precursors in hydrothermal process. The graphite flakes transformed into graphene oxide (GO) through oxidation by “Improved method” utilizing KMnO_4 as an oxidizing agent. The GO and composite material were studied by characterization techniques such as X-ray diffraction (XRD), Atomic force microscopy (AFM), Scanning electron microscopy (SEM) and Fourier transform infrared spectroscopy (FTIR). It exhibited the dispersion of thermally unstable tetragonal crystalline structure SnO nanoparticles of size range (25-53nm) on graphene sheet.

The resultant rGO/SnO composite obtained from different precursor solution ratio in hydrothermal process ($\text{SnCl}_2/\text{GO} = 1.1 \text{ mmol}/1\text{-}3 \text{ mg}$) and graphene film were coated for electrical measurements on pre-coated interdigitated electrodes alumina substrate, annealed at 250°C for 2 hrs.

Significant change in the current-voltage (I-V) characteristic of bare graphene observed on adding SnO nanoparticles, current drops from mA to μA . The current measured in composite material increase with the increase of graphene concentration in composite material. Resistance of rGO/SnO composite material (Precursor ratio= $1.1 \text{ mmol}/3 \text{ mg}$) decreased on raising temperature from $310 \text{ K}\Omega$ (25°C) to $297 \text{ K}\Omega$ (200°C).

TABLE OF CONTENTS

ACKNOWLEDGEMENT.....	I
ABSTRACT.....	II
TABLE OF CONTENTS	III
LIST OF FIGURES	V
LIST OF TABLES	VII
ABBREVIATIONS.....	VIII
1. INTRODUCTION.....	1
1.1 MOTIVATION.....	1
1.2 OUTLINES OF THESIS.....	2
2. LITERATURE REVIEW	4
2.1 GRAPHENE	4
2.2 GRAPHENE OXIDE (GO).....	6
2.3 METAL OXIDE NANOPARTICLES	7
2.4 TIN OXIDE (SnO₂ & SnO)	8
2.4.1 Crystalline Structure of Tin Oxide (SnO ₂ &SnO)	8
2.5 GRAPHENE DECORATED WITH INORGANIC NANOSTRUCTURE	9
2.5.1 Synthesis Route of Graphene / Inorganic Nanostructure Composite.....	12
2.5.2 Application of Graphene / Inorganic Nanostructure Composite.....	14
3. SYNTHESIS ROUTE AND CHARACTERIZATION TECHNIQUES	18
3.1 SYNTHESIS APPROACH TO GRAPHENE	18
3.1.1 Micromechanical exfoliation method.....	18
3.1.2 Chemical Exfoliation Method	19
3.1.3 Chemical Vapor Deposition (CVD)	20
3.1.4 Other Methods.....	21
3.2 CHARACTERIZATION TECHNIQUES	21
3.2.1 X-Ray Diffraction (XRD).....	21
3.2.2 Scanning Electron Microscopy (SEM).....	23
3.2.3 Energy- Dispersive X-Ray Spectroscopy (EDS).....	25
3.2.4 Atomic Force Microscopy (AFM)	26

3.2.5	<i>Fourier Transformation Infrared (FT-IR) Spectroscopy</i>	27
3.2.6	<i>Electrical Properties</i>	28
4.	EXPERIMENTAL WORK	29
4.1	SYNTHESIS OF GRAPHITE OXIDE	29
4.1.1	<i>Exfoliation of GO</i>	30
4.1.2	<i>Reduction of GO</i>	30
4.1.3	<i>Synthesis of SnO nanoparticles</i>	31
4.2	SYNTHESIS OF rGO/SnO COMPOSITE	33
4.3	SUBSTRATE PREPARATION FOR THE DEPOSITION OF COMPOSITE MATERIAL ..	34
4.3.1	<i>Thick Film Coating of Composite material on Substrate</i>	34
4.3.2	<i>Annealing</i>	35
5.	RESULT AND DISCUSSION	36
5.1	SYNTHESIS OF GRAPHENE OXIDE (GO) AND GRAPHENE (RGO):	36
5.1.1	<i>X-Ray Diffraction (XRD)</i> :	36
5.1.2	<i>Scanning Electron Microscopy (SEM)</i>	37
5.1.3	<i>Energy Dispersive Spectroscopy (EDS) of GO</i>	38
5.1.4	<i>Atomic Force Microscopy (AFM)</i>	39
5.1.5	<i>FT-IR analysis of GO and rGO</i>	41
5.2	CHARACTERIZATION OF TIN OXIDE AND GRAPHENE (RGO)/TIN OXIDE COMPOSITE	43
5.2.1	<i>X-Ray Diffraction (XRD)</i>	43
5.2.2	<i>Scanning Electron Microscope (SEM)</i> :.....	44
5.2.3	<i>Energy Dispersive Spectroscopy (EDS) of rGO/SnO Composite</i>	45
5.2.4	<i>FT-IR of rGO/SnO Composite</i>	46
5.3	ELECTRICAL PROPERTIES OF GRAPHENE AND rGO/SnO COMPOSITE	47
6.	CONCLUSION	50
	REFERENCES	51

LIST OF FIGURES

Figure 2-1: Number of Publications on Graphene Based Materials (2000 - 2014)[20]	5
Figure 2-2: Various structures formed by Graphene[36].....	6
Figure 2-3: Atomic configuration of (a)SnO ₂ and (b)SnO[67].....	9
Figure 2-4: Schematic representation of Fe ₃ O ₄ /rGO nanocomposite formation by in-Situ chemical deposition [69]	10
Figure 2-5: Schematic representation of substrate with interdigitated electrodes	15
Figure 2-6: Schematic illustration of graphene conductive surface for selective catalysis[34]	17
Figure 3-1: Making graphene by scotch tape method [71].....	18
Figure 3-2: Graphene Synthesis by Chemical Method [121]	20
Figure 3-3(a) X-Ray Diffraction STOE θ - θ (b) Schematic representation of X-ray diffractogram [133].....	23
Figure 3-4: (a) shows the JSM 6490LA SEM and (b)schematic of a SEM[134]	24
Figure 3-5: Schematic view of different signals generated on interaction of electron with sample [135]	25
Figure 3-6: Standard output spectrum of EDS [136].....	26
Figure 3-7: (a) Atomic Force Microscope JEOL (JSPM-5200)	27
Figure 3-8: (a) FTIR Spectrometer (b) Schematic diagram of FTIR.....	28
Figure 4-1: GO after reaction completion.....	29
Figure 4-2: Exfoliated GO in dispersion.....	30
Figure 4-3: (a) Process of reducing GO (b) reduced graphene oxide in suspension ...	31
Figure 4-4: Process of ultrasonicing the solution.....	31
Figure 4-5: Buchi autoclave setup for synthesis of nanocomposite	32
Figure 4-6: Synthesized SnO by hydrothermal process.....	32
Figure 4-7: Schematic of rGO/SnO synthesis.....	33
Figure 4-8: Al ₂ O ₃ substrate with combo shape interdigitated electrodes	34
Figure 4-9: rGO/SnO thick film on alumina substrate.....	35
Figure 5-1: XRD of (a) pristine graphite (b) GO.....	37
Figure 5-2: XRD of rGO.....	37
Figure 5-3: SEM images of GO layers	38
Figure 5-4: EDS spectra of GO sheet (Green peaks: C, O, S).....	38
Figure 5-5: AFM Images with height profile of GO nanosheet.....	41

Figure 5-6: FT-IR spectra of (a) GO and (b) rGO	42
Figure 5-7: XRD Patterns of SnO and rGO /SnO composite samples	43
Figure 5-8: SEM image of SnO particle	44
Figure 5-9: SEM images of rGO/SnO composite	45
Figure 5-10: EDS spectra of rGO/SnO Composite (Green peaks: C, O, Sn)	46
Figure 5-11: FT-IR of rGO/SnO Composite.....	47
Figure 5-12: I-V characteristic of (a)rGO (b)rGO/SnO composite	48
Figure 5-13: Temperature effect on rGO/SnO Composite	49

LIST OF TABLES

Table 2-1: Review of Graphene/Inorganic Nanostructure Composite	11
Table 5-1: EDS Result of GO	39
Table 5-2: EDS Result of rGO/ SnO Composite	46

ABBREVIATIONS

CNT	Carbon Nano Tubes
GO	Graphene Oxide
rGO	Reduced Graphene Oxide
HOPG	Highly Oriented Pyrolytic Graphite
CVD	Chemical Vapor Deposition
GCE	Glassy Carbon Electrode
ITO	Indium Tin Oxide
0D	Zero dimensional
1D	One dimensional
2D	Two dimensional
3D	Three dimensional
EDLCs	Electrochemical double layer capacitors
FWHM	Full Width at Half Maximum
eV	electron-volt
XRD	X-Ray Diffraction
SEM	Scanning Electron Microscope
AFM	Atomic Force Microscope
FT-IR	Fourier Transform Infrared
I-V	Current- Voltage
GRMs	Graphene related materials

1. Introduction

1.1 Motivation

The technological innovation and knowledge gathering are progress thoroughly in human history in a less or more exponentially. It has definitely been true after the enlightenment of development in natural science, helping in resources exploitation, creating new opportunities through new technologies in the western world.

We stand now in the beginning [1] of what appears to be one more revolution in the field of science and technology “Age of nano technology”. The growing interest in nanotechnology is because of nanostructure dimensions under 100nm. The strange properties of nanomaterials are connected to nano-dimensions, nanomaterials are those possessing at least one dimension below 100 nm [2]. Nano technology enables us to synthesize material at nanoscale, resulting the development of technology and tools which were never come in practice in the past centuries, some examples of nanotechnology advantages are cancer therapy with the help of nanoparticles [3] composite with enhanced performance[4, 5] and opens new windows in the field of materials, electronic and medicine.

The carbon nanostructures are the leading thread in the nanotechnology unfolding story, the particular development and study of which possesses considerably contributed in order to shaping the route to science taken place at nanoscale. Carbon is the chemical element, member of group 14 on the periodic table playing an important part in nature. The capability associated with carbon atoms in order to create complicated network is the basic to organic chemistry [6]. The nanostructures of carbon includes carbon nanotube, fullerenes, and recently reported single layer of graphite named graphene[7], These nanostructures forming various structures, but all are sp^2 hybridized carbon.

Graphene exhibiting unique properties and large surface area, is an attractive candidate for utilizing as a matrix to inorganic nanostructure [8]. Graphene properties can be further enhanced by functionalizing graphene sheet with different type of nanostructures. During the last few years ,various type of inorganic nanostructures including metal oxide such as TiO_2 [9] , SnO_2 [10] , Ce_3O_4 [11] , CuO [12] and

ZnO[13] have been effectively decorated on graphene sheet. The purpose of incorporating various types of functional materials through various techniques is to exploit the useful properties regarding graphene as well as graphene based composite. The substantial potential connected to graphene/inorganic composite in resolving several problems of today's, is visible from the efforts made on the exploring synthesis routes and material investigation in real life application, but research on graphene/inorganic composite still to be mature yet, and will be continue until the realization of using graphene in commercial product. The production of simple and measurable derivative linked to graphene "GO", well-off in oxygen functional groups encourage the researchers for incorporating various type of nanomaterials on the surface of single layer carbon sheet in order to fulfill commercial demands. The quality of these inorganic nanostructures decorated on graphene sheet will be ensured by the state of the art characterization techniques.

In order to study graphene/inorganic nanocomposite, different fabrication techniques are being adopted, but in our study we focused on the fabrication of rGO/tin oxide nanocomposite by very simple one step hydrothermal procedure. Tin oxide is probably one of the most significant materials being examined because of its chemical, physical and electronic properties. This research project is designed to prepared GO by method, producing small exothermic reaction, comparatively safer releasing less toxic gases and high yield of production with great oxidation of graphite. After that we will study the dispersion of unstable crystalline SnO on the surface of graphene, I-V characteristic of rGO/tin oxide nanocomposite thick film and effect of temperature on composite resistance.

1.2 Outlines of Thesis

Chapter 2: Summary of the literature related to graphene, graphene oxide (GO), tin oxides, graphene decorated with nanostructure, synthesis route and applications of graphene/inorganic nanostructure composite are discussed. In Chapter-3 describe the synthesis approach to graphene and characterization technique being used for the investigation of work performed. Describe the experimental work performed for the production of GO, rGO, SnO, rGO/SnO composite, substrate preparation with gold interdigitated electrodes and thick film coating on substrate in Chapter-4.

In Chapter-5 presented the result and discussion, in this regard effect of varying graphene concentration to SnCl₂ in hydrothermal process on I-V characteristic and resistance variation with temperature were also investigated. In Chapter-6 describe the conclusion of experimental work performed.

2. Literature Review

2.1 Graphene

Carbon demonstrates number of different structure like diamond and graphite having wide applications because of their hardness and softness respectively. Fullerenes[14] and carbon nanotubes [15] are recently discovered allotropes of carbon attaining great focus of physicist and chemist. Thus graphite (3D), nanotubes (1D) and fullerenes (0D) were known allotropes of carbon, among these the important two-dimensional form of carbon allotrope was missed.

Andre Geim and Kostya Novoselov from Manchester University, UK lead to revolution in this field in 2004. They used the top down approach using micromechanical cleavage technique to extract a single sheet from three-dimensional graphite named graphene [7].

Graphene is one atomic thick 2D structure of sp^2 bonded carbon atoms. This network of extended honey comb hexagonal crystal lattice arrays having 0.142nm range of carbon to carbon [7, 16, 17].The unit cell consists the pair of carbon atoms and around any atom is invariant under 120° rotation .The mechanical stability of the carbon sheet is highly contributed by single s orbital and double in-plane p orbital with every atom [18] .

Graphene is being considered building block of three-dimensional graphite ,zero-dimensional buckyball as well as one-dimensional carbon nanotube, stacking of graphene sheets gives graphite, rolling carbon nanotube and wrapping buckyball [17] as shown in Fig2-2.

Graphene reveals outstanding electrical, optical, thermal as well as mechanical properties. Because of this, graphene based materials attain larger focus of the researchers, and the numbers of publications related to GRMs are increasing continuously shown in Fig.2-1.

Some of the important properties of graphene are:

- 1) Perfect graphene with infinite plane exhibits zero band gap and zero effective mass electrons where both bands conduction and valance meet. This specific tends

to make graphene a great anomalous product which does not work as either semiconductor or metal [19].

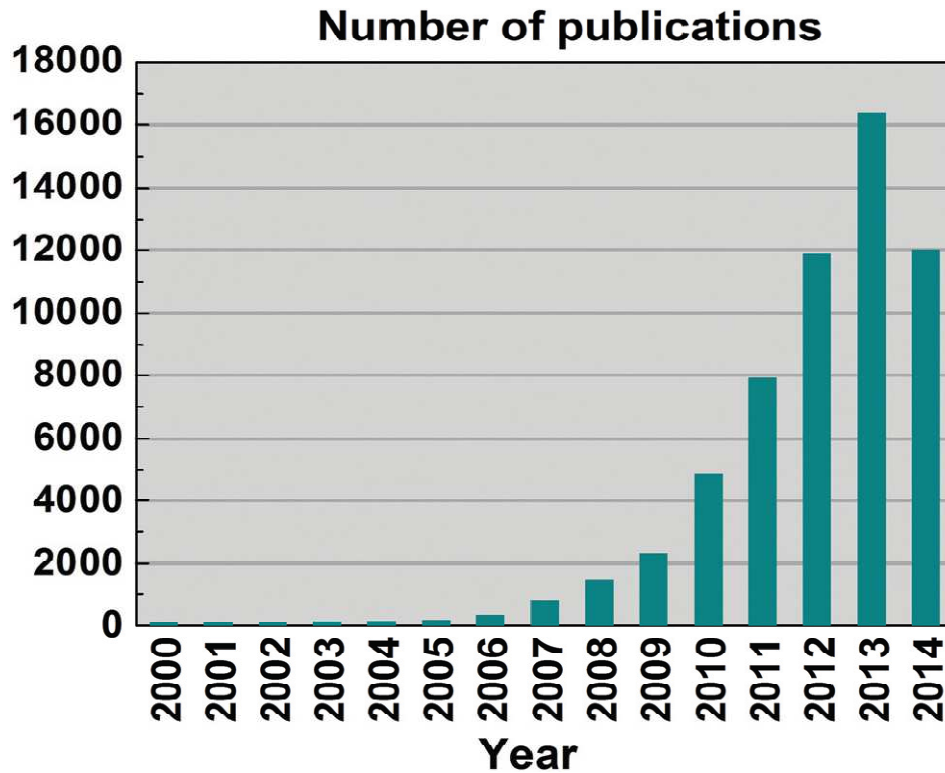


Figure 2-1: Number of Publications on Graphene Based Materials (2000 - 2014) [20]

- 2) Because of particular planar structure of graphene makes it possible to insert microsphere with diameter size larger than few hundred nanometers on graphene sheet[21].
- 3) As compared to carbon nanotube, graphene offer larger surface area $\sim 2600 \text{ m}^2 \text{ g}^{-1}$ enhance interfacial contact to other components, but larger surface area of graphene having one drawback of irreversible agglomeration [22, 23].
- 4) Resistivity regarding Graphene is about ($10^{-6} \Omega \text{ cm}$) considered to be the substrate having least resistivity on room temperature, the electron transport like in graphene has not practically observed in any kind of semiconductor, as a result graphene offers turned out to be consider the most non-superconducting conductive material [24].
- 5) Aside from higher carrier mobility, graphene is essential invisible, absorb merely 2% of incident light irrespective of wavelength over the visible spectrum. [25].

- 6) Graphene reveals quantum hall effect [7, 26]
- 7) Graphene nanosheet shows larger electron mobility $\sim 200000 \text{ cm}^2 \text{ V}^{-1}\text{s}^{-1}$ [27].
- 8) Graphene manifests extraordinary thermal conductivity $\sim 5000 \text{ Wm}^{-1}\text{K}^{-1}$ because of phonon which is beneficial for electronic application [28].
- 9) Graphene single layer present extraordinary mechanical properties with young modules 1 TPa and 42 Nm^{-1} of strength breaking, so considered is the strongest material and because of this property it makes graphene possible to fabricate various devices [29].

Since graphene has outstanding properties, makes it perfect candidate to use in various areas like optoelectronics [30], spintronics [31] touch displays [32] chemical sensors [33], catalysts [34]. Polymer composite based on graphene offering enhance properties like mechanical strength and high heat and electrical conductivity [35].

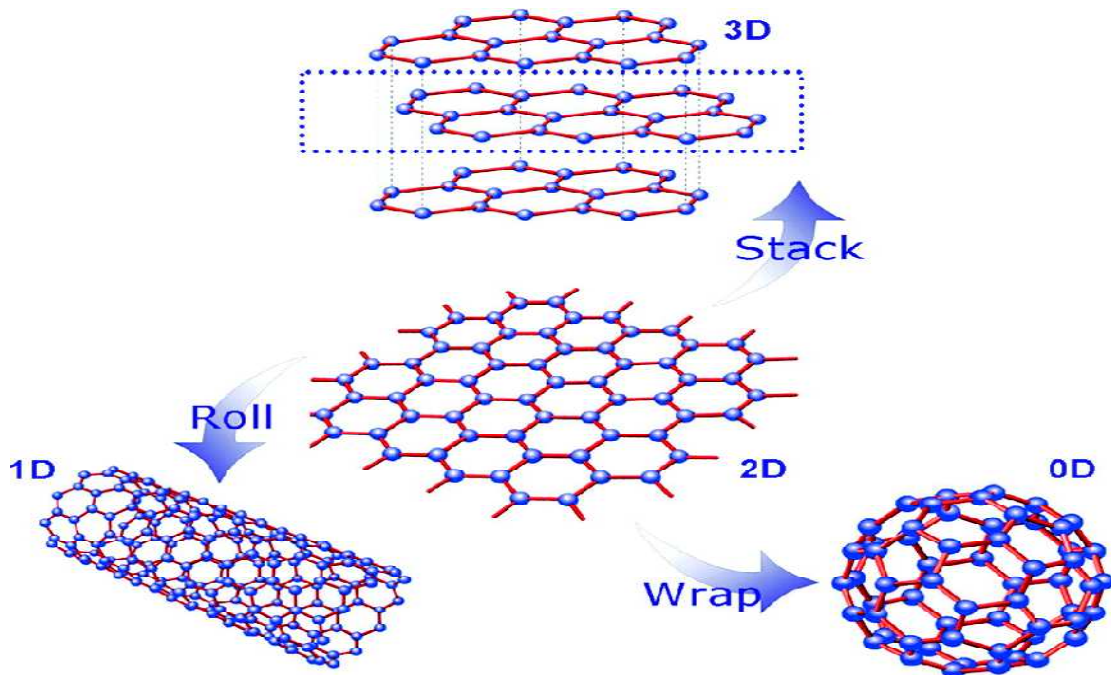


Figure 2-2: Various structures formed by Graphene [36]

2.2 Graphene Oxide (GO)

Graphene oxide is the monolayer with oxygen rich nanomaterial. The most common way to produce is the well-controlled oxidation of graphite [37], then by exfoliation of graphite oxide produce graphene oxide.

In 1859, Brodie for the first time presented the synthesis of graphite oxide (GO) with the help of adding small quantity of potassium chlorate to graphite slurry with fuming

nitric acid [38], Staudenmaier in 1898 enhanced this method by introducing concentrated sulfuric acid together with fuming nitric acid, these small changes in protocol results make it more practical [39]. The most common way to use nowadays for the oxidation of graphite is demonstrated by Hummer in 1958 introduced a relatively safer method by using KMnO_4 and NaNO_3 with concentrated sulfuric acid [40]. In 2010, Tour makes further efforts for the improvement of oxidation by introducing phosphoric acid replacing nitric acid [41]. Graphite oxide through oxidation by this method results in more oxidized. This method can be used for bulk production of graphite oxides because of small exothermic reaction involvement and safer, do not releasing toxic gases. Graphene oxides behave hydrophilic because of hydroxyl (OH) group attachment to the graphene oxide (GO) nanosheet surface [42], and because of the hydrophilicity property of GO, it's become easy to coat uniform thin film on substrate for different type of microelectronics application [43]. Commercially available graphene oxide having application in the area of solar cell [44], polymer composite [45], biomedicine [46], transparent conductive film [47], paper like material [48] and electromechanical devices [49].

2.3 Metal Oxide Nanoparticles

Metal oxide plays a vital role in numerous areas connected with chemistry, physics and material science disciplines. The metal element has the ability to form substantial variety connected to oxide component [50]. These can undertake variety of structural geometries through an electronic structure that could demonstrate their identity as an insulator, semiconductor or metal. The primary goal in nanotechnology is to develop nanostructure/nanoarrays exhibiting some sort of properties that should be different from bulk. Oxide nanoparticles with limited size in addition of corner high density offer distinctive chemical as well physical properties [51]. The sizing of the particles are usually supposed to put effect on three significant groups of any material fundamental properties, the primary one is structural features, specifically the cell parameters and symmetry of lattice [52]. The 2nd group of properties having size related consequence of oxides material is electronic properties. The material having nanostructure shows confinement effect because of atom like discrete electronic states, that can be viewed as accompanying rise in strength of oscillator, some sort of superposition regarding bulk like state [53]. The third group size related consequence

of oxide material with in simple classification, several oxides gives less reactivity and wide band gap with in bulk state [54].reduction in oxides particle size effect the size of band gap as well chemical reactivity [55, 56].

2.4 Tin oxide (SnO_2 & SnO)

Nano materials possess excellent attention because of their interesting physical, electrical, chemical and magnetic properties which might be different from those associated with bulk state.

Tin oxide is probably one of the most significant materials being examined nowadays for the reason of their chemical, physical as well as electronic structure study. This investigating study mostly concern to tin dioxide may be because of SnO decomposition at elevated temperature; however SnO and SnO_2 usually coexist either because of SnO_2 reduction or SnO oxidation. Yaun et al.[57] reported that SnO is the outmost oxide phase of Sn which transform eventually into SnO_2 phase after certain annealing. Hart et al.[58] presented his study on the Sn foil oxidation process, from amorphous tin oxide to crystalline SnO and then to SnO_2 (high valence oxide). Tin oxide is n-type semiconductor material, with SnO_2 energy gap of 3.6 eV and SnO energy gap lies between 2.5 and 3 eV ,smaller as compared to SnO_2 [59]. SnO is metastable and formed Sn_2O_3 in certain amount on raising temperature to 600 K [60]. SnO_2 is highly stable offer substantial carrier density and facilitate tremendous concentration of intrinsic along with stoichiometric-violating vacancies linked to help their electrical conductivity [61]. Tin oxide has wide range of application such as photosensors[62] ,photovoltaic devices [63],electrode materials [64] and specially for gas sensors [65] .

2.4.1 Crystalline Structure of Tin Oxide (SnO_2 & SnO)

The SnO and SnO_2 both have tetragonal crystalline structure at room temperature and pressure. An important form of naturally taking place of SnO_2 is cassiterite, a rutile structure of SnO_2 has a tetragonal unit cell, where every Sn atom is encased by six oxygen in the octahedral array and every oxygen encased by three Sn atom in the planer. Perhaps the most probably positive feature of SnO_2 associated with the many of its application are considered is the changes associated that may takes place in its surface composition. Material electronic structures are greatly affected by the

variation causes reducing surface structure. Reducing surface Sn^{+4} with Sn^{+2} will results Sn 5s state that lies in the band gap in addition to lowering work function [66] while in case of tetragonal SnO , each Sn atoms comprise pyramids structure with four oxygen atoms. The Sn atoms falls on pyramids vertices along with oxygen square basis. Edge sharing of the pyramids results formation SnO structure layer having Sn at the vertices laying alternately below and above them. Fig.2-3 shows the SnO and SnO₂ atomic configuration, Oxygen atom presented by large sphere while tin by small one. Dashed line in case of SnO₂ present the formation of Octahedral arrays while square based pyramids formation in case of SnO.

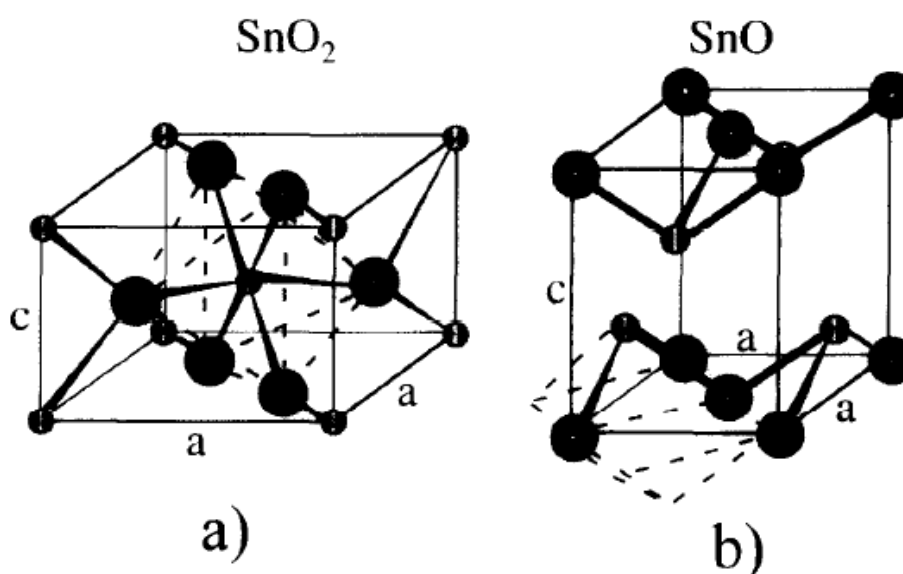


Figure 2-3: Atomic configuration of (a)SnO₂ and (b)SnO [67]

2.5 Graphene decorated with inorganic Nanostructure

Over the last decade, nanostructure of distinct size and shapes attain the greater focus of researchers due to its exciting properties. Various nanoparticles of inorganic compounds including metals, metal oxide and others are being used for graphene/inorganic composite in order to enhance graphene properties. This nanocomposite exhibits different structure and morphology depends upon the synthesis process. The generally recognized process to the synthesis regarding graphene decorated with inorganic nanostructure is the attachment of metal ions having positive charged on the GO functional groups because of polarized bonds.

These connections leads to redox reaction along with the creation of nucleation sites, then ultimately contribute to the development of nanostructure on graphene sheet. An example of Fe₃O₄/rGO formation [68] where Fe²⁺ ions are primary attached with the surface functional groups of graphene oxide sheet is shown in Fig.2-4. The GO behave as an oxidizing agent ,successfully raising oxidation state of Fe²⁺ to Fe³⁺ results the formation of Fe₃O₄ on the surface of rGO sheet with in alkaline environment.

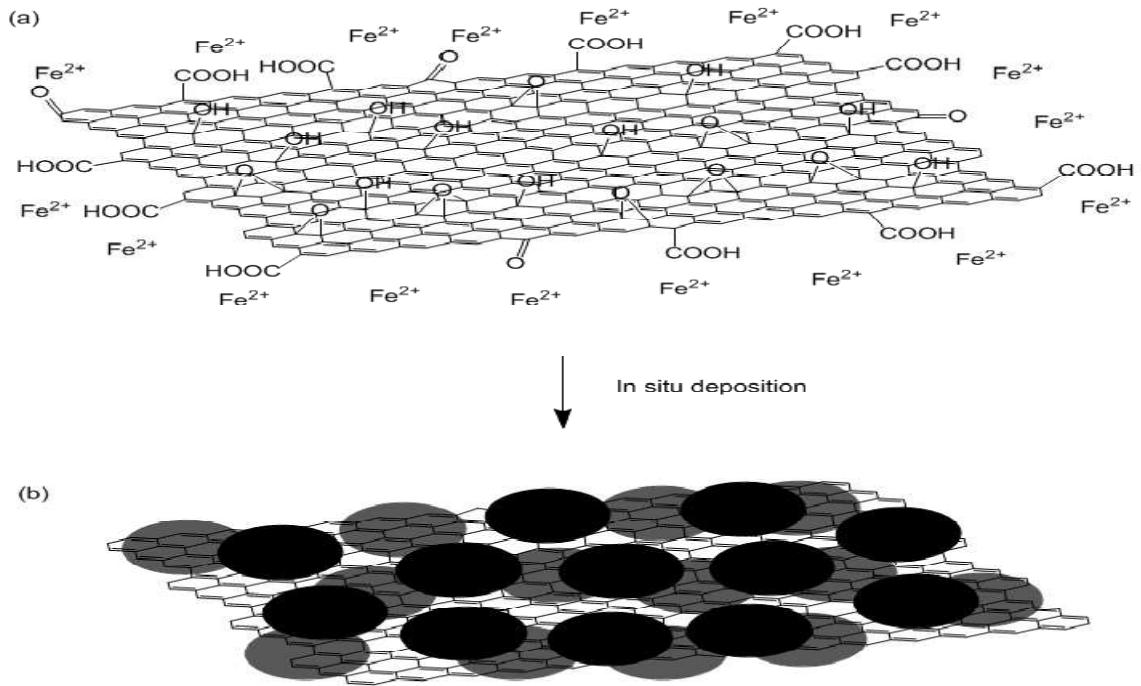
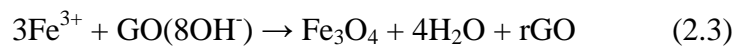
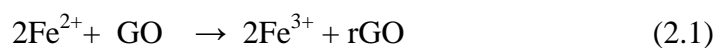


Figure 2-4: Schematic representation of Fe₃O₄/rGO nanocomposite formation by in-Situ chemical deposition [69]

The whole process can be represented in three simple equations



Regarding fabrication of metal/graphene composite are usually developed via reduction of metal ions and GO at the same time [70].

Nanoparticles incorporation with rGO sheet might be via physisorption , chemisorptions, covalent interaction, van der Waals and electrostatic interaction [12, 71].the main advantages of nanostructure attached to rGO decrease interaction of

attraction between sheets results minimization of aggregation [72] ,furthermore enable nanocomposite with uniform dispersion in polar solvents because of nanostructure trace quantity on rGO basal plane [69].

Making use of GO to be a support pertaining inorganic nanostructure like metals and metal oxide a number of distinct composite are already synthesized, some of them are listed in table 2-1.

Table 2-1: Review of Graphene/Inorganic Nanostructure Composite

Nanostructure	Dimension	Synthesis Route	Application	Reference
Fe ₃ O ₄	12.5nm	Reaction in Gas Liquid interface	Anode for Li-Ion batteries	[73]
Mn ₃ O ₄	10nm	Ultrasonication	Supper capacitor	[74]
SnO ₂	10 nm	Microwave	Mercury (II) detection	[75]
TiO ₂	4 to 5 nm	Sonochemical	Photocatalysts	[76]
ZnO	Dia~90nm Length ~3um Nanorods	Hydrothermal	Gas sensor, solar cell	[77]
SnO ₂	4 to 5nm	Microwave autoclave	Anode for Li-Ion batteries	[78]
Ag ₂ O	45nm	In-Situ oxidation	Supercapacitor	[79]
SnO ₂	3 to 5 nm	Hydrothermal	Catalytic degradation	[80]
La ₂ Ti ₂ O ₇	Nanosheet integrated	Expansion in UV radiation	Photocatalyst	[81]
Ni	Single layered	Electrolysis Ni plating	Sensors, electrode	[70]
Pd	5 to 7 nm	Laser irradiation	CO oxidation	[82]
Pt	5 to 7 nm	Laser irradiation	CO oxidation	[82]

2.5.1 Synthesis Route of Graphene / Inorganic Nanostructure Composite

2.5.1.1 In-Situ Chemical Synthesis

This method is really an effective way for the development graphene/inorganic nanostructure composite. The primary step for the formation of composite by in-situ technique is the interaction between metal ions having charge positive and cloud of negatively charge electron around Oxygen atom attaining GO. Nanostructure attached uniformly to graphene sheet following the reaction because of the fact that Oxygen atoms are tends to be spread evenly in beginning of GO sheet. Several metal oxide for example SnO₂ and Fe₃O₄ developed on the surface of reduced graphene oxide even at room temperature [69, 83], however if the reaction temperature is increased, calcinations by raising temperature might be able to be removed like Graphene/SnO₂ [84].reduction of graphene oxide always remains challenging therefore in order to conform the complete reduction of graphene oxide some time reducing may be employed. Considering the example of using ammonia solution and hydrazine for the synthesis of Ag/Graphene composite [85].Whenever sheets of graphene are utilized directly, some sort of stabilizer agent become necessary in addition to higher reaction temperature in order to promote formation of nanostructure just like synthesis of Fe on graphene [86].

2.5.1.2 Microwave Heating

Microwave heating technique for the nanostructure synthesis is considered to be more dependent on the properties of molecules as well process condition rather than traditional heating. This technique is widely used for the synthesis of oxides nanoparticles like SnO₂, ZrO₂, and CeO₂ having substantial monodispersity [87].Providing highly localized and short time thermal treatment with the help of microwave heating technique results very fine particle, size lies in between 15-35 nm in nanocrystalline regime [88].Definitely graphene sheet plays a vital role in the fabrication of Graphene/inorganic- nanostructure with particle size less than 10 nm through microwave heating [89]

2.5.1.3 Hydrothermal and Solvothermal

Hydrothermal synthesis is basically an effective route for the formation of distinct inorganic nanostructure at well controlled temperature and pressure. This kind of synthesis technique ruled out the problems regarding high temperature and lengthy

reaction time in comparison with typical chemical processing [90]. It has been accepted as an environment friendly process for the reason of reaction using a medium of aqueous solution completed in an autoclave closed system. This process may also be used for the production of highly pure, crystalline and homogeneous powder [91], however it's not compulsory to use pure aqueous solution, some other type of solution like ethanol can be used for promoting dispersion like graphene oxide [92]. Autoclave employed in hydrothermal process is a closed system, therefore enhancing temperature as well as increased pressure within vessel. Over the critical pressure of aqueous solution promotes thermodynamically unsound dissolution of compound the thermal energy and high pressure applied by autoclave fracture the compound into particles in nano size [93]. CuO/Graphene [12], ZnO/Graphene [77], SnO₂/Graphene [80] are being synthesized through this technique.

If the reaction medium solution is not based on aqueous then process is known as solvothermal.

Absolute ethanol has been used as a medium for reaction in the formation of SnSb/Graphene [94]. Using the method similar like hydrothermal SnO₂/Graphene was prepared through reaction at liquid-gas interface [95].

2.5.1.4 Electro-deposition

Electrodeposition technique makes possible the formation of film with controlled and precise thickness, with the addition of speed up the polymerization process that can be controlled by current density [96]. Glassy carbon electrode (GCE) are usually used in this technique for coating of graphene oxide, then electrode with GO coating are allowed to submerge in salt solution, by applying potential cycle results to rGO by GO reduction, and oxidation of metal to metal oxide. ZrO₂/graphene [97] is one of the examples prepared by using this technique.

Since graphene oxide is considered to be hydrophilic and will not be removed from the surface of GCE when taking place in electrolytes, however it is challenging to develop homogeneous dispersion of graphene within solvent because of tending irreversible agglomeration by means of van der Waals interaction and π - π stacking in graphene sheet. Cyclic voltametry are being used for the growth of nanostructure on

graphene using this technique. Ag/Graphene [98] are prepared by using this method in salt solution.

2.5.2 Application of Graphene / Inorganic Nanostructure Composite

2.5.2.1 Sensor:

Different analytical techniques are used for the sensing application of matter (organic & inorganic) having high sensitivity and excellent response to very low limit of target material [99], but it is difficult to use in field for monitoring because of its high cost, complicated and complex instruments, trained manpower and lot of time consuming [100]. In comparison, electrochemical analysis is an alternate method for detection containing features of simple instrumentation, less time consuming, low cost, small power requirements and simple operating procedure extensively utilized in the application of chemical sensors, biosensors and gas sensors [85, 101, 102]. Since inorganic nanostructure exhibits large surface area, mechanical strength, high thermal stability, chemical stability and substantial electrical features when decorated on graphene sheet offers an interesting composite for the application of gas sensor. Qianqian Lin et al. [103] reported the fabrication of graphene/SnO₂ nanocomposite by the use of hydrothermal technique and the composite material shows response for 10 to 50 ppm of NH₃ gas at room temperature. The response magnitude was defined by the eqn. 2.4.

$$S = (Z_{\text{NH}_3} - Z_{\text{air}}) / Z_{\text{air}} \times 100 \quad (2.4)$$

Z_{NH_3} = impedance in NH₃ gas

Z_{air} = impedance in air

Giovanni et al. [104] used SnO₂/rGO as a sensing material towards NO₂, and it is observed that the composite response towards NO₂ strongly depends upon the ratio of SnO₂ loading on reduced graphene oxide. The resistance of graphene/SnO₂ increased several orders of magnitude compared to rGO.

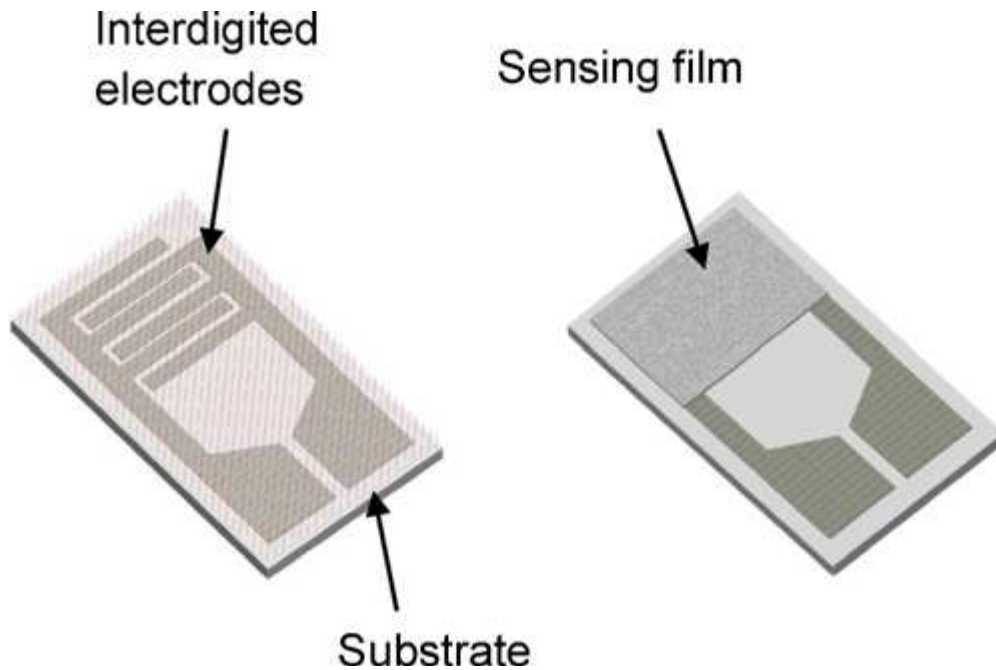


Figure 2-5: Schematic representation of substrate with interdigitated electrodes

2.5.2.2 Supercapacitors:

Supercapacitor which is also known as ultracapacitor. It is different from conventional capacitor exhibiting high energy density. In contrast to conventional capacitor supercapacitor are designed with special electrodes and electrolyte for the energy storage through ion adsorption in limited package. Supercapacitor was introduced publically for the first time in 1957 and becker filed patent on this discovery [105], restoring high capacitance through double layer processing on carbon having high surface area. There are two categories of supercapacitors regarding energy storage, one is known as electrochemical double layer capacitors (EDLCs) and the another one is pseudocapacitor. EDLCs usually carry high surface area and electrochemically stability. Since carbon based material offers excellent electrical conductivity and electrochemical stable with high surface area, so widely used as a electrode in EDLCs [106] Several researchers prepared Supercapacitors from the material through decorating nanocrystal such as Co_3O_4 [11] RuO_2 [107] SnO_2 [108] on graphene layer preventing restacking of graphene sheets. These entire graphene based composite remarkably improved the specific capacitance.

2.5.2.3 Anode for Lithium Ion batteries

Lithium ion batteries based on graphite material experienced bad charge/discharge efficiency as a result possess weak power efficiency. In most of applications similar to hybrid or electric vehicles required high power in some occasion like overtaking with high speed, and that enhance dissipation of heat in the cell and so increasing battery aging. The battery power efficiency was greatly improved by the use of electrode based on graphene published their results through papers. Graphite based battery provides 372 mAhg^{-1} while the graphene provides higher capacity for energy storage just above 600 mAhg^{-1} because of accommodating capability of Li ions on its both sides. Recent study shows the improvement in energy storage capacity in the range of 700 to 4000 mAhg^{-1} with the use of graphene/metal oxide composite [109]. The battery function in many application is charge and discharge repeatedly and important point is weakening of storage capacity during these cycles. Graphene based inorganic nanostructure offers far better efficiency as compared to individuals [12]. Nanocrystal decorated on graphene sheet minimize agglomeration during repetitions of charge/discharge resulting electrodes with high electrical conductivity and surface area forming excellent carrier mobility.

2.5.2.4 Photocatalysts:

The rapid increases in the world population are giving rise to pollution in environment because of organic waste from various sectors such as industries, agriculture and human waste. Millions of people all over the world annually faced to death because of disease born by contaminated water and around four billion people having no, or very small approach to clean water [110]. These organic pollutant required degradation, so great attention were given to decontamination in the last decay irrespective of its chemical nature and its state (gas or liquid) of target to process [111, 112]. When light is allowed to fall on photocatalysts, as a result electron excited from valence to conduction band, therefore creating electron hole pair. When photocatalyst interact with water these $e^{-}h^{+}$ pair start a chain of reaction on photocatalyst surface producing hydroxyl radicals ($\text{OH}\bullet$) as well as superoxide radicals anion ($\text{O}\bullet^{-}$), therefore oxidized the organic pollutant situated near the surface through radicals generated on surface [113]. A number of semiconductors such as zinc oxide and titanium dioxide are used as photocatalysts, but one problem link to these photocatalysts is the fast recombination of $e^{-}h^{+}$ within surface of semiconductors results poor efficiency. In

this regard graphene based composite attain greater attention to overcome the problem of e^-h^+ recombination. Zhou and Zhu et al. [114] conformed that TiO_2 nanoparticles dispersed on graphene sheet improved photocatalytic process. In this process sun light were allowed to fall on the composite material for the purpose of methylene blue degradation within water. When UV light falls on TiO_2 /graphene resulting excitation of TiO_2 So e^-h^+ pair generated in TiO_2 , shifting to graphene sheet, hunt through dissolved oxygen and avoiding e^-h^+ recombination.

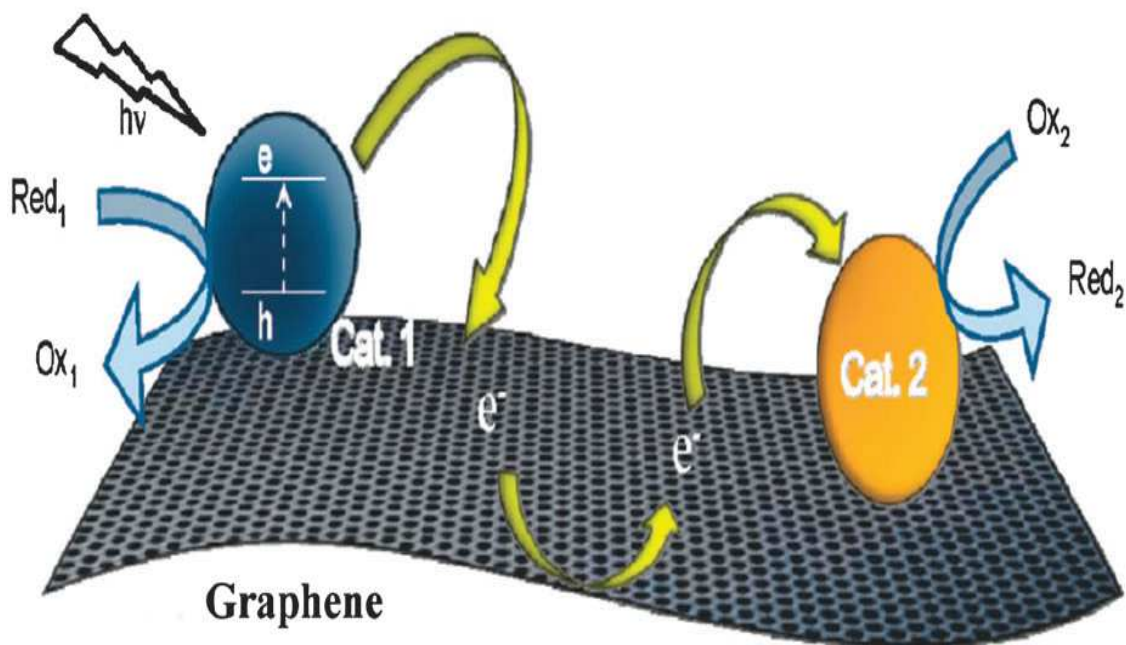


Figure 2-6: Schematic illustration of graphene conductive surface for selective catalysis [34]

Besides TiO_2 /graphene, other semiconductors such as ZnO /graphene [115], SnO_2 /graphene [116] etc photocatalysts studied for the application of water pollutant decomposition.

3. Synthesis Route and Characterization Techniques

3.1 Synthesis Approach to Graphene

Geim and Novoselov was awarded Noble prize in 2010 by successful discovery of graphene in 2004, after the reorganization of graphene for the first time in 2004 many effort were made by improving the synthesis route to produce defect free graphene sheets. Some of the key synthesis routes of graphene are summarized here below.

3.1.1 Micromechanical exfoliation method

Probably the most simple and easy way for the production of pristine graphene is graphite exfoliation with the help of scotch tape using the phenomenon “exfoliation and cleavage”. Graphene layers are stalked together in graphite by week van der wall forces, mechanical or chemical energy are provided by exfoliation and cleavage in order to overcome these week bonds. This method using top down approach was reported for the first time by Novoselov et al. in 2004 [7],initially one mm thick sheet of highly oriented pyrolytic graphite (HOPG) were dry etched in oxygen plasma to several 5 μ m deep mesas, then peeled apart layer-by-layer using scotch tape.

Perfect or near to perfect graphene layer with the drawback of low production rate can be produced by this method [7, 117].



Figure 3-1: Making graphene by scotch tape method [71]

3.1.2 Chemical Exfoliation Method

The most popular technique for the synthesis of graphene is through oxidation and exfoliation of graphite which overcome the drawbacks related to micromechanical exfoliation method such as low production rate and difficulties in controlling process. This kind of technique entails acidic solution for the oxidation of graphite, after occurring of graphite oxidation, breaking straight into distinct layers resulting graphene oxide sheets. Following the reduction of GO by use of some sort of strong reducing agent consequently produce quality graphene layers. The particular oxidative treatment method allows to enhance interlayer spacing among graphene sheets within graphite [118, 119]. Benefit of graphene producing by means of this method is the mass production without usage of costly equipments, furthermore its colloidal solution can be easily utilized for making composite materials. On the other hand synthesis of pristine graphene would be difficult to produce due to the fact of complete reduction of carbon lattice are not achievable by mean of this method, In addition conduction level is week as compared to the that of graphene produced through scotch tape technique.

Various procedures such as Hummer, Hoffman and Staudenmaier methods are being used for the oxidation of graphite [40] Oxidation of graphite crystal occurs by the use of sulfuric acid along with hydrogen peroxide solution which in turn in the sheet results hydroxyl as well epoxide groups, and carbonyl and carboxylic groups at the edge of sheet [120]. These sheets are hydrophilic because of functional groups disturbing the van der waals forces among sheets. Separation of sheets in this particular situation may be accomplished by mean of mild sonication. [121].

The suspension of graphene sheets are stable for lengthy period of time when dispersed in water, this is possible because of the carboxylic and hydroxyl groups creating negative charge on the sheets giving rise to electrostatic repulsion among the sheets.

A difference of color in graphene oxide on dispersion also observed changing from abundant dark colored to some strong yellow color as oxidation enhanced. Solid dried GO appears brown. By nature graphene oxidation is insulating, so can be reduced to graphene to reinstate carbon lattice in conductive state.[121] . In case of utilizing GO for the purpose of composite synthesis, following the reduction of GO by employing treatment through thermal anneal [121], UV illumination [122], hydrazine [23] or

hydroquinone [123]. Utilizing these kinds of techniques various type of devices are already produced such as solar cells [124].

As already stated that it is very difficult to completely reduced GO, for this reason film prepared by employing GO following reduction could have lesser conductivity in comparison with pristine graphene [125].

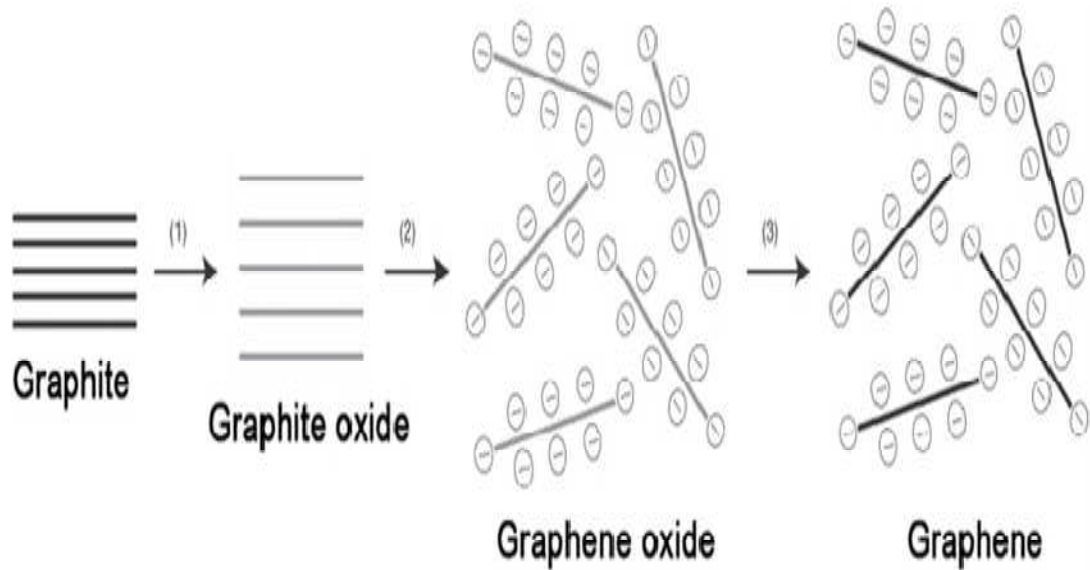


Figure 3-2: Graphene Synthesis by Chemical Method [121]

3.1.3 Chemical Vapor Deposition (CVD)

Besides the scotch tape technique, several researchers presented alternate ways in approach to synthesize graphene. After discovery of graphene experimentally, Somani et al. in 2006 developed few layers graphene by utilizing nickel sheet, and about 35 numbers of layers were estimated with the help of SEM [126]. This method exposed sites for graphene synthesis, despite the fact various problems such as uniformity and thickness controlling would have to be resolved. Then using CVD process, several groups succeeded in achieving graphene film on nickel foil with thickness in the range of 1-2 nm [127]. The CVD process provides exceptional continuous film of graphene, while restricted the size of film to the silicon terrace width on growing from silicon carbide. Transferring process in graphene synthesis by chemical vapor deposition is placed one of the key challenges to overcome.

3.1.4 Other Methods

Lot of approaches are being used till date for the synthesis of graphene ,such as unzipping of carbon nanotube gives graphene nanoribbons [128].

Although by comparing with normal graphene sheet nanoribbon exhibit diverse morphological as well physical properties with distinctive electronic properties because of quantum confinement [129] Liquid phase exfoliation [130] and solvothermal [131] approach are also reported for the graphene synthesis.

3.2 Characterization Techniques

3.2.1 X-Ray Diffraction (XRD)

X-Ray diffraction (XRD) is versatile characterization tool, used for phase analysis, measurement of stresses in coatings, particle size, crystal structure and orientation. In Fig.3-3 (a) particular X-ray diffraction STOE θ - θ applied are shown. In this process, typically x-ray of known wavelength at certain angle of incident hit the specimen. The beams diffracted from the atoms of sample results constructive or destructive interference. If diffracted rays are out of phase resulting destructive and will cancel each other, In another case if diffracted beams are in phase, produce constructive interference as shown in Fig.3-3(b).This kind of interference depends upon the spacing between parallel planes associated with atoms of material that's distinct for various materials [132] .A detector are used to collect signal intensity and describes quantitatively by means of Bragg's law proposed by William Lawrence Bragg and William Henry Bragg in 1913 in reflected X-rays. They observed that those crystals, at certain particular wavelength and incident angle, produce intense peak of reflected radiation, known as Bragg peak.

$$2d \sin\theta = n\lambda \quad (3.1)$$

Where,

d = interplanar spacing

θ = diffraction angle

λ = wavelength of x-ray

n = order of diffraction

X-Ray Diffraction has three different techniques

1. Lawe method
2. Rotating crystal method
3. Powder method

X-Ray machine installed in our school is STOE diffractometer, Germany operated at 40 KV and 40 mA was used for the conformation of average particle size and crystal structure. This X-Ray diffractometer is powder type and X-Ray used are $\text{CuK}\alpha$ (1.5418 \AA) is produced at point and the diffracted beam intensities were detected with a counter. It was insured that the specimen, X-Ray source and counter are all coplanar.

In this study, X-Ray diffractometer (XRD) was utilized for graphene oxide (GO) with 2θ range $5-30^\circ$, SnO_2 and rGO/ SnO_2 composite with 2θ range between 20° and 70° .

The particle size was calculated by Scherrer formula using full width at half maximum (FWHM).

The average particle size is given by

$$\tau = 0.9\lambda / \beta \cos\theta \quad (3.2)$$

Where

λ is the wavelength of incident X-Rays

β is half width of peak

θ is diffraction angle

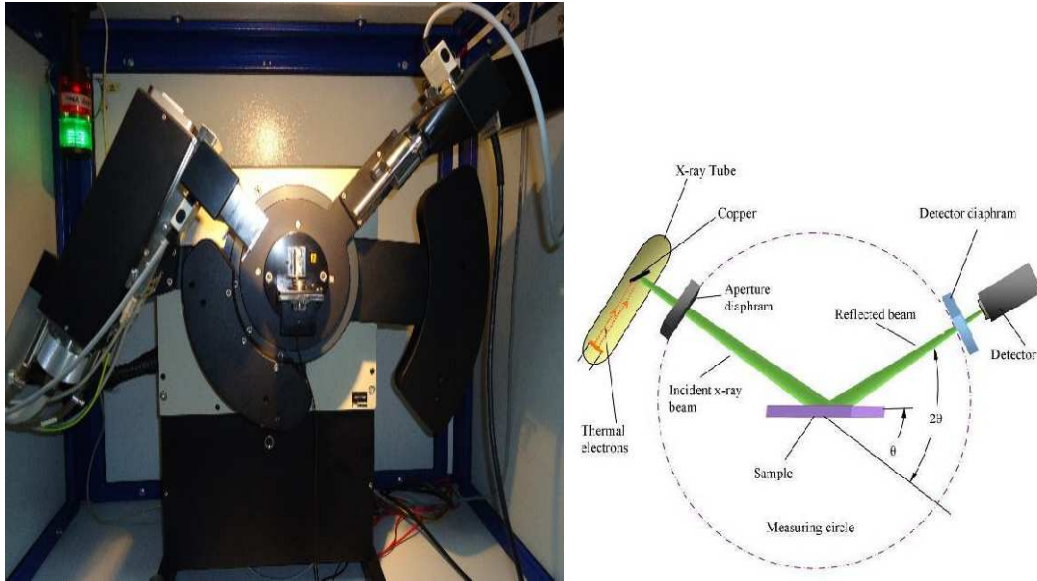


Figure 3-3(a) X-Ray Diffraction STOE θ - θ **(b)** Schematic representation of X-ray diffractogram [133]

3.2.2 Scanning Electron Microscopy (SEM)

Scanning electron microscopes have high magnification and high depth of focus, therefore used widely to examine the microstructures thoroughly. Most of the data are received from a selected area of the surface of the sample, results a 2-dimensional image displaying spatial variations in these properties. In conventional SEM techniques, magnification ranging from 20 X to 30,000 X, spatial resolution of 50 to 100 nm, areas in scanning mode in range of 1 cm to 5 microns in width can be imaged. An electron beam is emitted from cathode gun carrying considerable amount of kinetic energy in Kev. This high energy electrons are focused with the help of objective and condenser lenses. The focused beams are used to scan the particular rectangular area of the sample. As electron beam interacts with the atoms in the sample, due to dissipation of its energy a variety of signals like back scattered or secondary electrons are generated. These signals are detected with the help of highly specialized detectors. Further the signals are amplified to obtain magnified image of the surface with the resolution in the range of nm. As the number and speed of reflected electrons from the specimen surface are different, so different grey scaled image of SEM generated. In SEM image, element with high atomic number appears brighter as compared to the element with low atomic number.

In our research project SEM analysis is done with the help of JEOL SEM (JSM 6490LA).

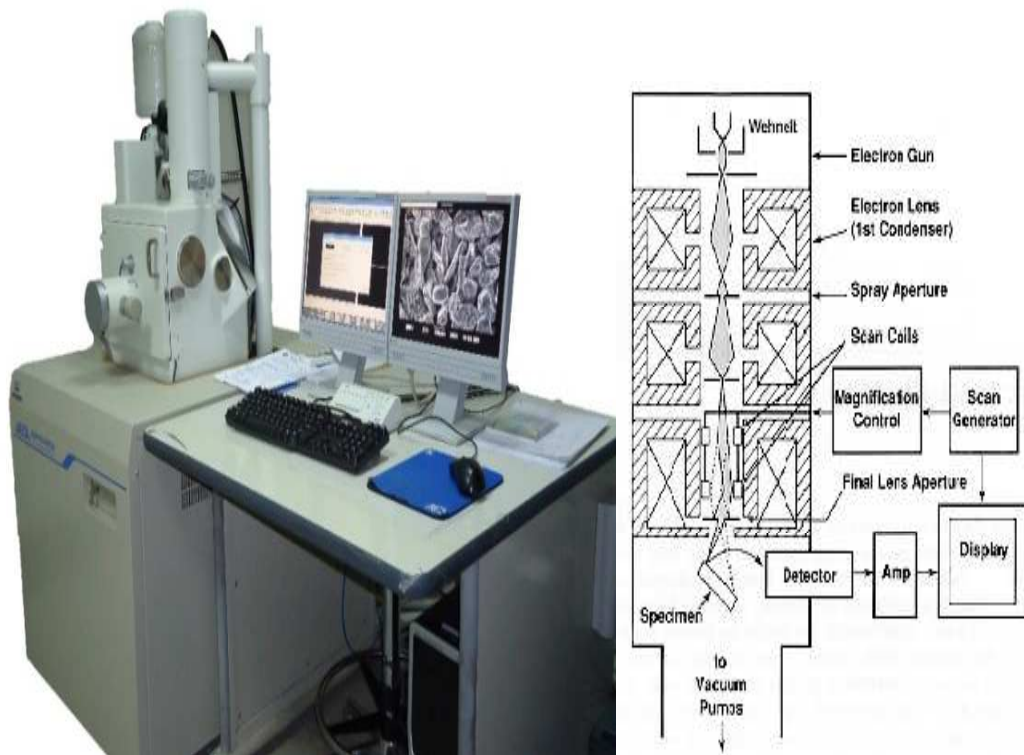


Figure 3-4: (a) shows the JSM 6490LA SEM and (b) schematic of a SEM [134]

There is no doubt that no other instrument is compatible with the SEM to study solid materials. The SEM is critical in all fields needing the characterization of solid materials, besides of its geological applications, it has vast and scientific and industrial applications. Most SEM's are easy to operate, needing minimum sample preparation with rapid acquisition. Modern SEM is capable to generate digital data in digital format, which are highly portable.

SEM has also some limitations. Sample must be solid and should be able to fit in microscope chamber. Mostly, stability of sample required vacuum of 10^{-5} - 10^{-6} torr.

Most SEM used solid state X-ray detector (EDS), very fast and easily utilize, have poor energy resolution and sensitivity to element present in low abundances, compared to wavelength dispersive x-ray detectors (WDS) on most electron probe microscope (EPMA).

For conventional SEM study , an electrical conductivity coating must be applied to electrical insulating samples unless the instrument is capable of operating in low vacuum mode [135].

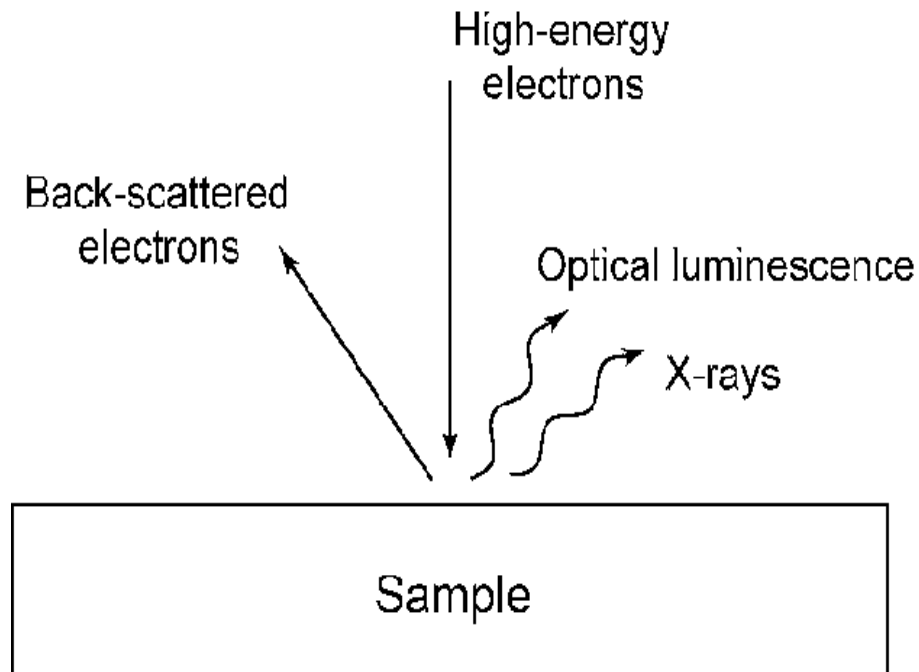


Figure 3-5: Schematic view of different signals generated on interaction of electron with sample [135]

3.2.3 Energy- Dispersive X-Ray Spectroscopy (EDS)

EDS analyses are used to attain elemental maps or spot chemical analysis by utilizing characteristic x-rays generated from the sample. X-rays are generated by inelastic collision of the high energy incident electron with the electron in discrete orbital of the atom in sample which on de excitation, jumps to lower energy state, yielding x-ray that are of fixed wavelength depends on the difference in energy levels of electron in different shells for given element, thus each element that is “excited” by the electron beam, produce characteristic x-ray. These x-rays generated from different element are collected by specialized detector, measure its energy and then compare it with the standard value of different elements makes possible to find out different element in sample. In addition to qualitative analysis, quantitatively measurement of the elements can be made by mean of calculating counts at these particular energies.

Beside to qualitative analysis, the elements could be measured quantitatively simply by mean of calculating counts at this particular energies as shown in Fig.3-6.

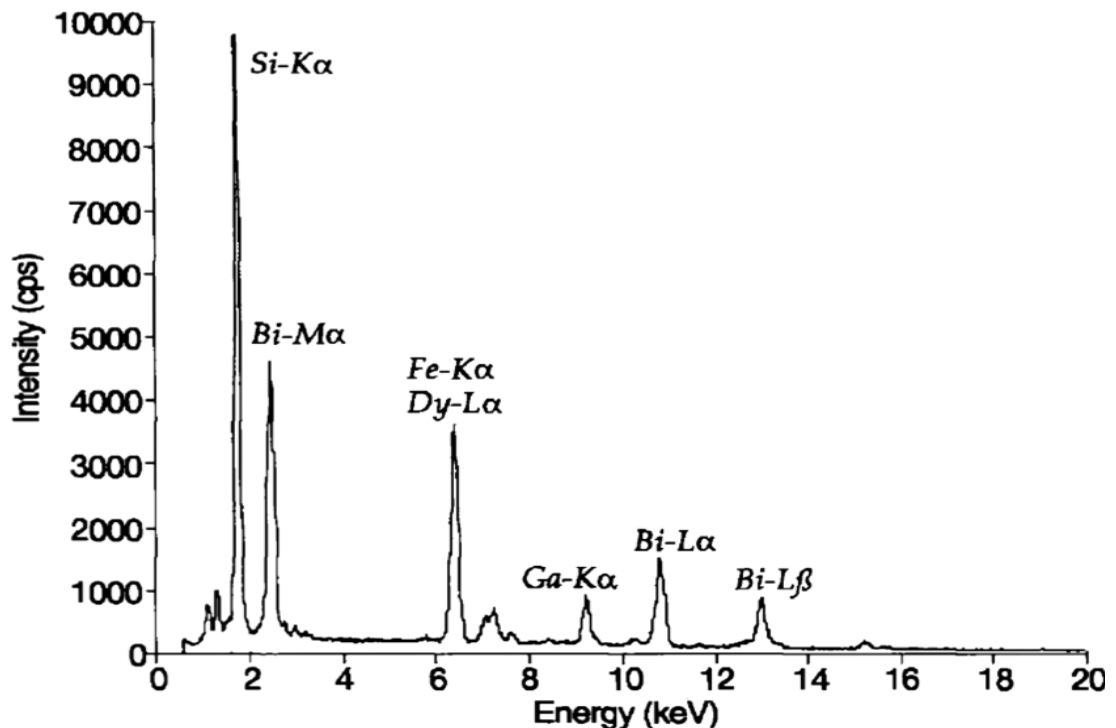


Figure 3-6: Standard output spectrum of EDS [136]

3.2.4 Atomic Force Microscopy (AFM)

Although optical microscope and electron microscope are powerful tools for the imaging of object with the magnification up to 1000X in case of optical microscope, and upto 100,000X for electron microscope. The image obtained by these conventional microscope provides two dimensional information (horizontal axis), do not describe vertical dimension. Unlike conventional microscope, AFM measures forces between the surface and sharp probe falling at short distance (0.2-10 nm) from each other providing 3D profile of the specimen. The ability to magnify image in X, Y & Z axis by AFM is of great importance as compared to conventional microscopes. The principle of AFM working is to produce van der waals forces of repulsion between the atoms on the tip with cantilever and the surface of the sample during the scanning. As the tip approaches near within the distance of few angstroms to the surface, results deflection due to repulsive force. AFM incorporate scanner exhibiting

piezoelectric characteristic that is operated by feedback controller, which in turn scans the tip on the surface of specimen, also preserve constant distance of the AFM tip from the sample surface. The deflection because of the surface of the sample with varying topography is monitored with the help of optical lever. For this purpose a laser diode is utilized to allow the beam which is reflected back from cantilever to position sensitive photodiode.

In this research project AFM JEOL (JSPM-5200) was used.

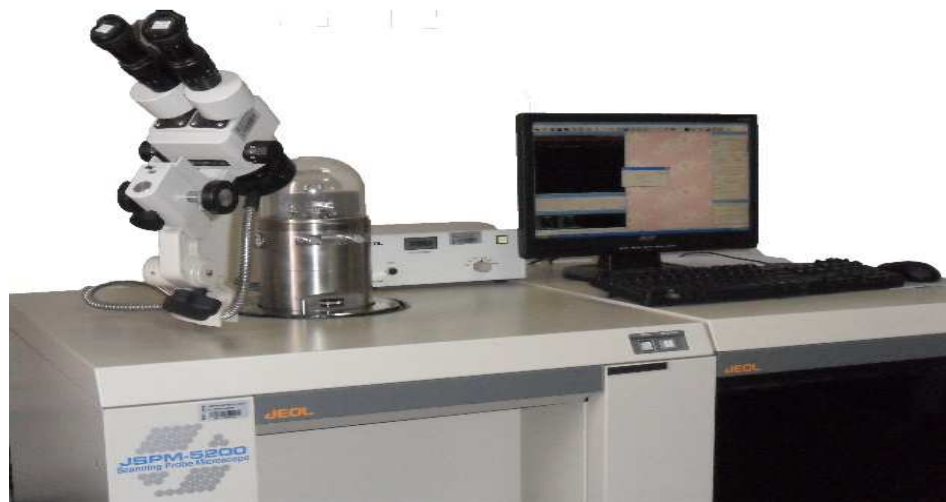


Figure 3-7: (a) Atomic Force Microscope JEOL (JSPM-5200)

3.2.5 Fourier Transformation Infrared (FT-IR) Spectroscopy

Fourier transform infrared (FTIR) is measurement technique used for collecting IR spectra such that radiation is guided through interferometer. FTIR spectra present the detail information regarding functional groups present within the sample, and therefore utilized mostly in semiconductor industry to find out the presence of atom impurity or involvement of any other dopant. It tells all the info regarding functional groups relevant to oxygen and carbon bonding.

The function of interferometer is to split IR radiation into two beams, and to make one of the beams have to travel optical distance that would be different than the optical distance travel by another one, creating alternating interference fringes.

FTIR spectrometers are low cost as compared to other conventional spectrometers, because it is easy to build an interferometer than the fabrication of a monochromator, furthermore FTIR technique makes faster the measurement of a single spectrum because of information regarding all frequencies are received at once, makes possible to collect several samples and then average together. This results in an increase in sensitivity.

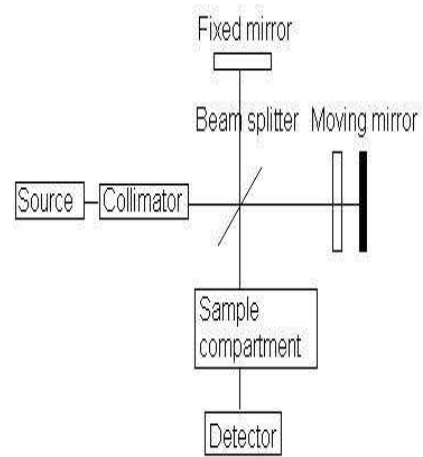


Figure 3-8: (a) FTIR Spectrometer (b) Schematic diagram of FTIR

3.2.6 Electrical Properties

I-V represent the relationship in the form of chart or graph between the electric current (I) and voltage (V) applied across the circuit or any device. In our case we plot the graph, measuring current across the known material fabricated device using Agilent (34401A) digital multimeter, when applied voltage by using Keithly source meter (2400-C) with increasing step of 1 volt. We also measured the change in the resistance of the composite material by varying temperature from 25 °C to 200 °C.

4. Experimental Work

4.1 Synthesis of Graphite oxide

Graphite oxide was prepared by using “ Improved method” [41]. 1 gram of graphite flake was mixed in the mixture of 9:1 concentrated $\text{H}_2\text{SO}_4/\text{H}_3\text{PO}_4$ (90:10 ml) and stirred through magnetic stirrer. 6 g of potassium permanganate (KMnO_4) was added slowly into the mixture under stirring. The mixture was stirred at 35-40 °C for 6 hours producing slightly exothermic reaction. After that mixture was heated up to 50 °C for 12 hrs under stirring. Finally, the solution was allowed to cool down to room temperature and poured into 400 ml ice cubes of de-ionized water with 5 ml hydrogen peroxide (H_2O_2) in order to complete the reaction. The solution color change from dark pink to yellow. Washed the mixture with 1 M HCl and then with de-ionized water many time till the pH of supernatant reached to 7.



Figure 4-1: GO after reaction completion

4.1.1 Exfoliation of GO

Exfoliating of graphite oxide was ended by sonicating the GO dispersion for one hour. The stable yellow-brown solution produced showing its stability for long period of time, can be used for reductions and other applications. The nanoparticles were dried at 40 °C for 24 hrs under vacuum.



Figure 4-2: Exfoliated GO in dispersion

4.1.2 Reduction of GO

Some portion of the prepared graphene oxide was reduced using hydrazine hydrate for comparison. Briefly 1ml of hydrazine hydrate were mixed into exfoliated GO dispersion, the solution was heated up to 90 °C in oil bath for 12 hrs under stirring by Teflon covered stirrer. The change in the color of solution to clearly black from brown, indicating reduction of GO. The black solid precipitate subsequently washed with methanol and de-ionized water and dried at 40 °C for 24 hrs under vacuum.



Figure 4-3: (a) Process of reducing GO (b) reduced graphene oxide in suspension

4.1.3 Synthesis of SnO nanoparticles

SnO nanoparticles were prepared by autoclave hydrothermal process, SnCl_2 acts as a precursor for SnO. 1.30 g of $\text{SnCl}_2 \cdot 2\text{H}_2\text{O}$ was mixed with 50ml de-ionized water through magnetic stirrer. Adding 1.30 g of urea $\text{CO}(\text{NH}_2)_2$ and 0.7 ml HCl (36-38%) into the solution under continuous stirring for 30 minutes, followed by ultrasonicing the mixture for one hour, obtained translucent solution. All the chemicals used were of analytical grade.



Figure 4-4: Process of ultrasonicing the solution

After that transferred right the resultant solution into 125 ml Teflon lined stainless steel autoclave keeping 120 °C reaction temperature for 8 hrs and cooled to room temperature naturally. The SnO nanoparticles subsequently washed with ethanol and de-ionized water and dried at 60 °C for 24 hrs under vacuum.

In this research project Buchi autoclave setup were used shown in Fig.4-5.



Figure 4-5: Buchi autoclave setup for synthesis of nanocomposite

The role of urea in the solution is to decompose into NH_3 and CO_2 within the solution, subsequently used to neutralized HCl by NH_3 dissolved in water forming NH_4Cl , promoting the formation of SnO from SnCl_2 [108]

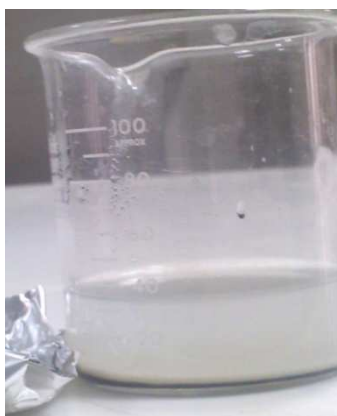


Figure 4-6: Synthesized SnO by hydrothermal process

4.2 Synthesis of *rGO/SnO* composite

The *rGO/SnO* composite was formed by autoclave hydrothermal process. GO and SnCl_2 acts as a precursor for the formation of *rGO/SnO* composite. Right amount of GO was mixed in 50 ml de-ionized water and sonicated for one hour. Adding 1.30 g $\text{SnCl}_2 \cdot 2\text{H}_2\text{O}$ into GO dispersion and stirrer through magnetic stirrer, followed by mixing 1.30 g urea and 0.7 ml HCl under continuous stirring for 30 minutes, the final mixture was treated by ultrasonication for one hour. After that transferred right the resultant solution into 125 ml Teflon lined stainless steel autoclave keeping 120 °C reaction temperature for 8 hrs and cooled to room temperature naturally. No doubt that reaction was performed in acidic environment makes synthesis of composite broaden and useful for further applications. The *rGO/SnO* composite was subsequently washed with ethanol and de-ionized water and dried at 60 °C for 24 hrs under vacuum. The different experiments were named *rGO/SnO*-1, *rGO/SnO*-2 and *rGO/SnO*-3 on the basis of precursor solution (SnCl_2/GO : 1.1 mmol/1 mg, 1.1 mmol/2 mg, 1.1 mmol/3 mg) respectively being used in hydrothermal process. The whole process can be shown in the diagram below.

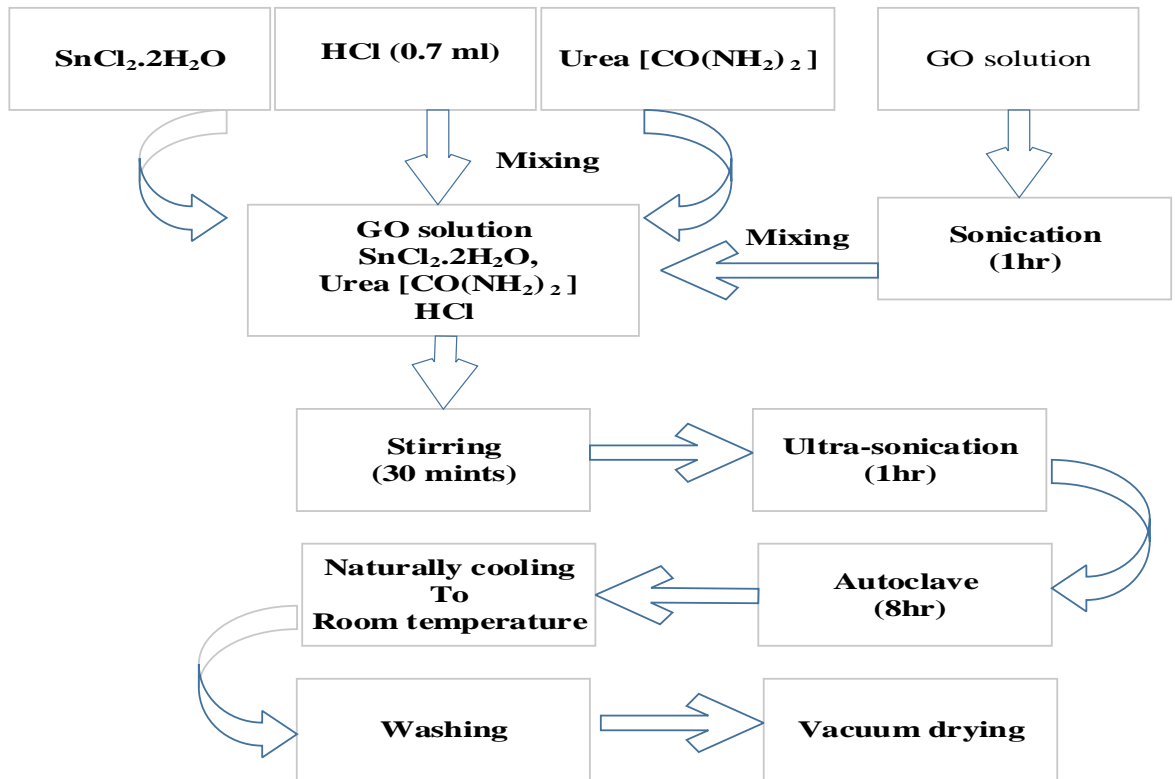


Figure 4-7: Schematic of *rGO/SnO* synthesis

4.3 Substrate preparation for the deposition of composite material

The ceramic alumina (Al_2O_3) substrate $13 \times 8 \times 2$ mm was put into mask made of stainless steel. Gold combo shape interdigitated electrodes were deposited on alumina substrate through thermal evaporating for the application of fabricating composite material on electrodes and for further electrical connection. The width and gap between pairs of electrodes is 0.75 mm, advantage of interdigitated electrodes is to makes possible the detection of low ppm level.



Figure 4-8: Al_2O_3 substrate with combo shape interdigitated electrodes

4.3.1 Thick Film Coating of Composite material on Substrate

An aqueous paste of rGO/SnO composite powder material was prepared by adding rGO/SnO (5 mg/0.5 ml) into de-ionized water. Thick film of composite material was painted on the substrate having interdigitated electrodes using soft brush and dried in air at $80\text{ }^\circ\text{C}$.



Figure 4-9: rGO/SnO thick film on alumina substrate

4.3.2 Annealing

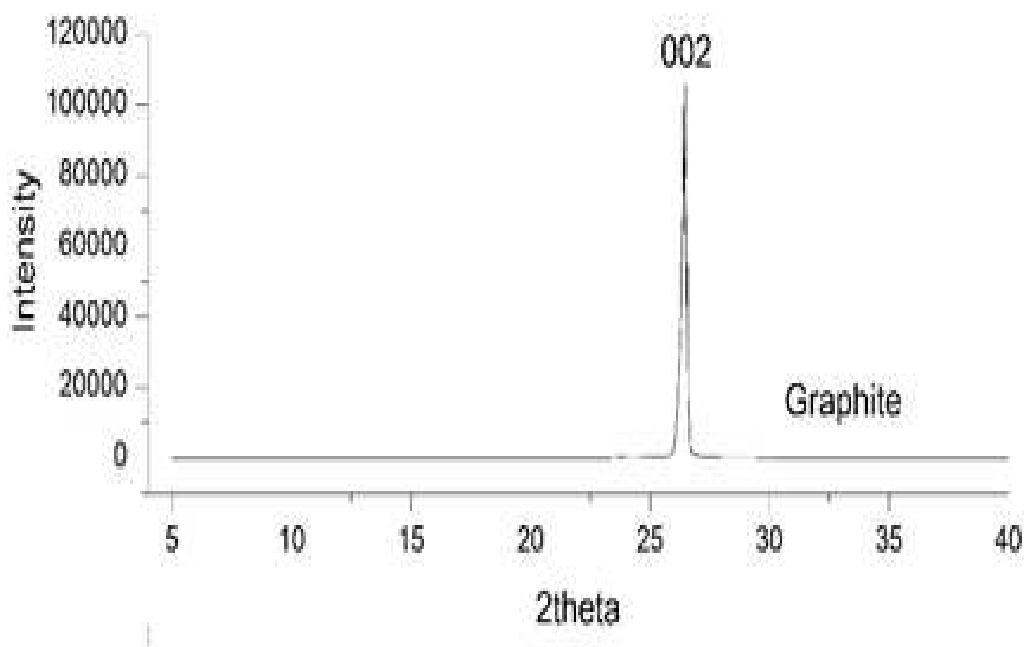
After depositing thick film, the sample was annealed at 250 °C at the heating rate of 2 °C for 2 hours in NaberthermGmbH N17/HR-400V Muffle heating furnace for the purpose of film microstructure and texture stability, and cooled down to room temperature naturally.

5. Result and Discussion

5.1 Synthesis of Graphene Oxide (GO) and Graphene (rGO):

5.1.1 X-Ray Diffraction (XRD):

We confirmed the average crystalline structure of GO and rGO with the use of X-Ray diffraction and compared with pristine graphite. The pristine graphite flake before oxidation shows high degree of crystalline with intense diffraction peak (002) at $2\theta = 26.4^\circ$ having d-space 0.34 nm as shown in Fig.5-1(a). However the XRD pattern of GO showing its diffraction peak (002) relatively low intensity shifted to $2\theta = 10.4^\circ$ with no peak at 26.4° with interplanar spacing greater than 0.6 nm indicating fully oxidation of graphite in Fig.5-1(b). Since oxygen atoms sandwich between layers on oxidation of graphite increase interlayer spacing, weakening the van der Waals interaction among layers, makes easy the exfoliation by sonication [137].



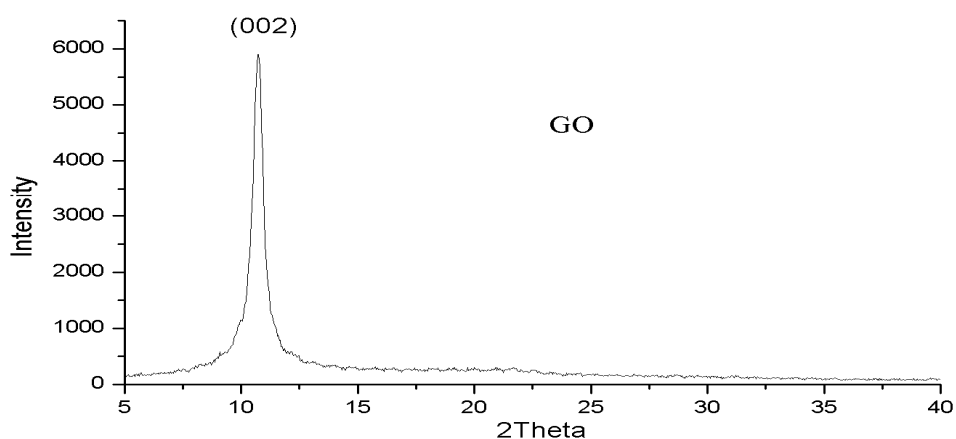


Figure 5-1: XRD of (a) pristine graphite (b) GO

When some portion of the GO sheets was reduced chemically by use of hydrazine hydrate into rGO sheets for comparison, the diffraction peak (002) once again shifted to 26.4° from 10.4° in Fig.5-2.

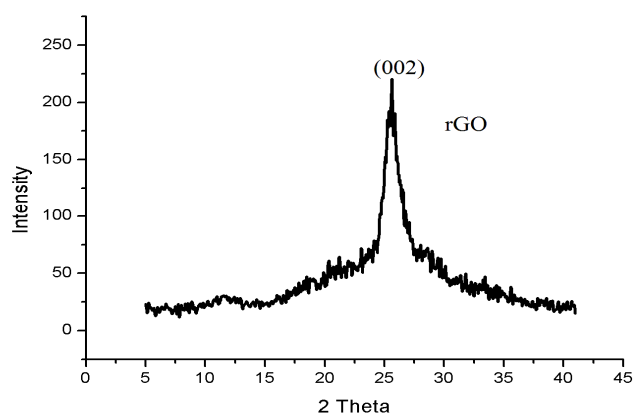


Figure 5-2: XRD of rGO

5.1.2 Scanning Electron Microscopy (SEM)

Specimen of graphene oxide (GO) for SEM were prepared by drop of dispersed GO in water on silica substrate. Graphene oxide (Single or multi-layer) from the oxidation and exfoliation of graphite as seen in SEM image Fig 5-3. A closely packed “tiling” of graphene oxide platelets having an even contrast was observed on the substrate.

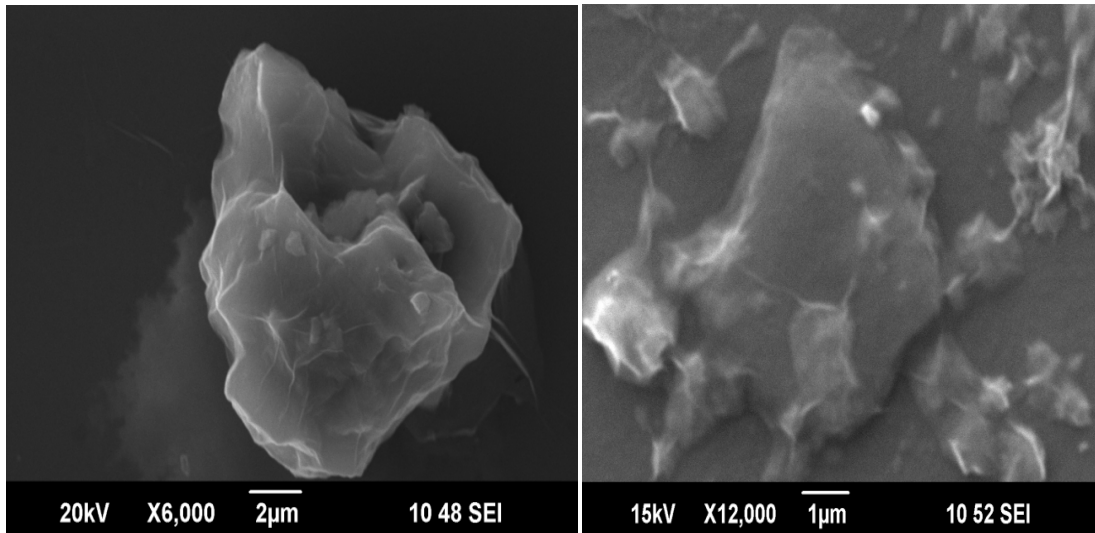


Figure 5-3: SEM images of GO layers

5.1.3 Energy Dispersive Spectroscopy (EDS) of GO

The elemental composition of resultant GO sheet was confirmed by EDS analysis. The EDS analysis spectrum clearly represent the C:O ratio nearly equal to 1:1 coincides with the experimental results reported in literature [138]. In addition to C and O, 0.8% S despite of excessive washing was also observed listed in table 5-1.

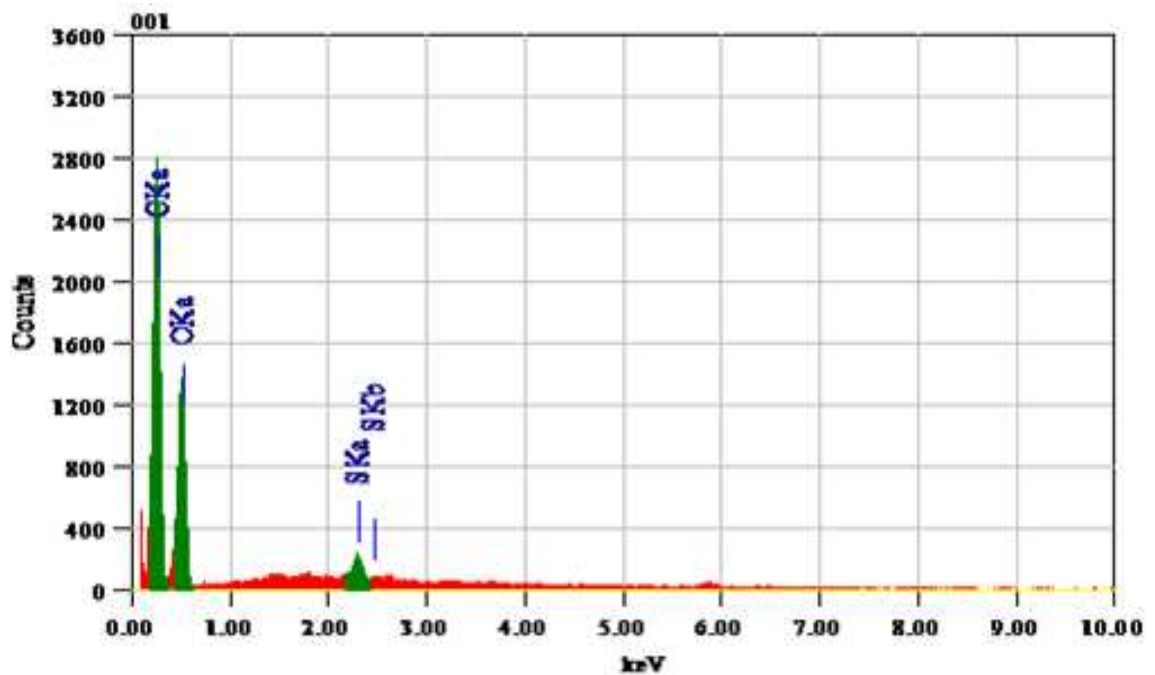


Figure 5-4: EDS spectra of GO sheet (Green peaks: C, O, S)

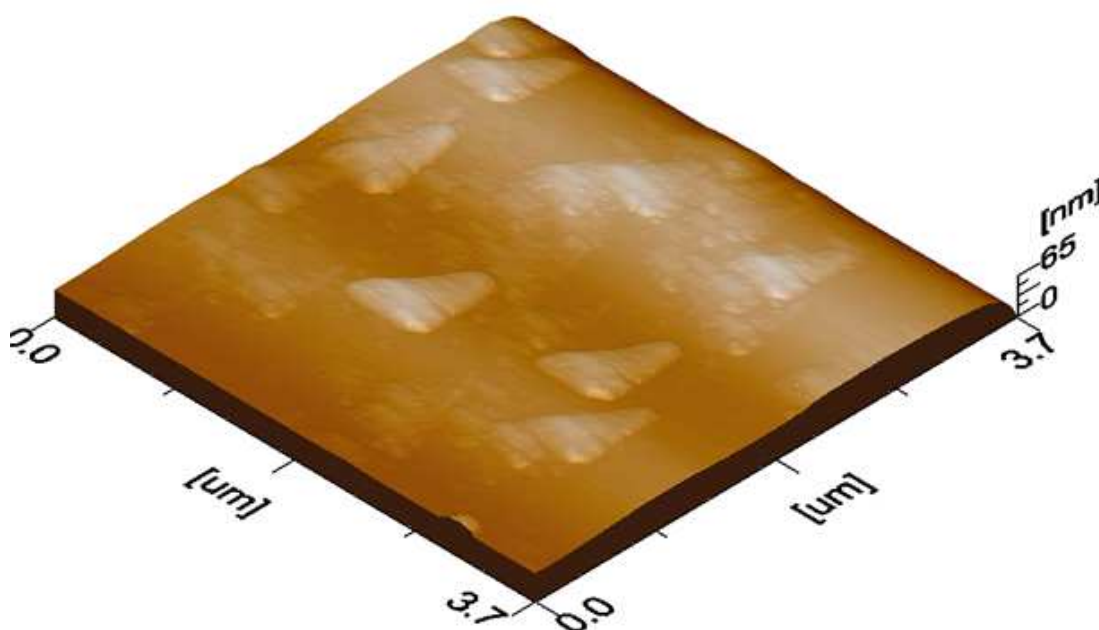
Table 5-1: EDS Result of GO

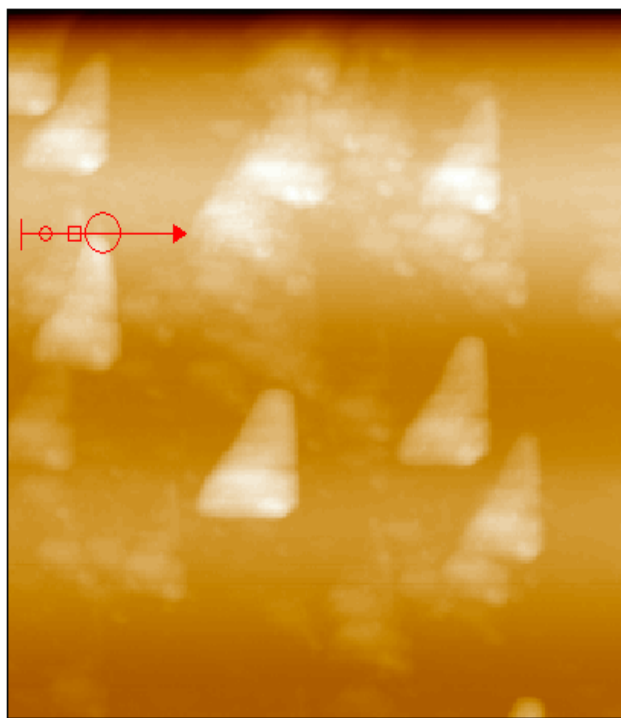
Element	(KeV)	Atom%
C K	0.277	50.46
O K	0.525	48.73
S K	2.307	0.81
Total		100


5.1.4 Atomic Force Microscopy (AFM)

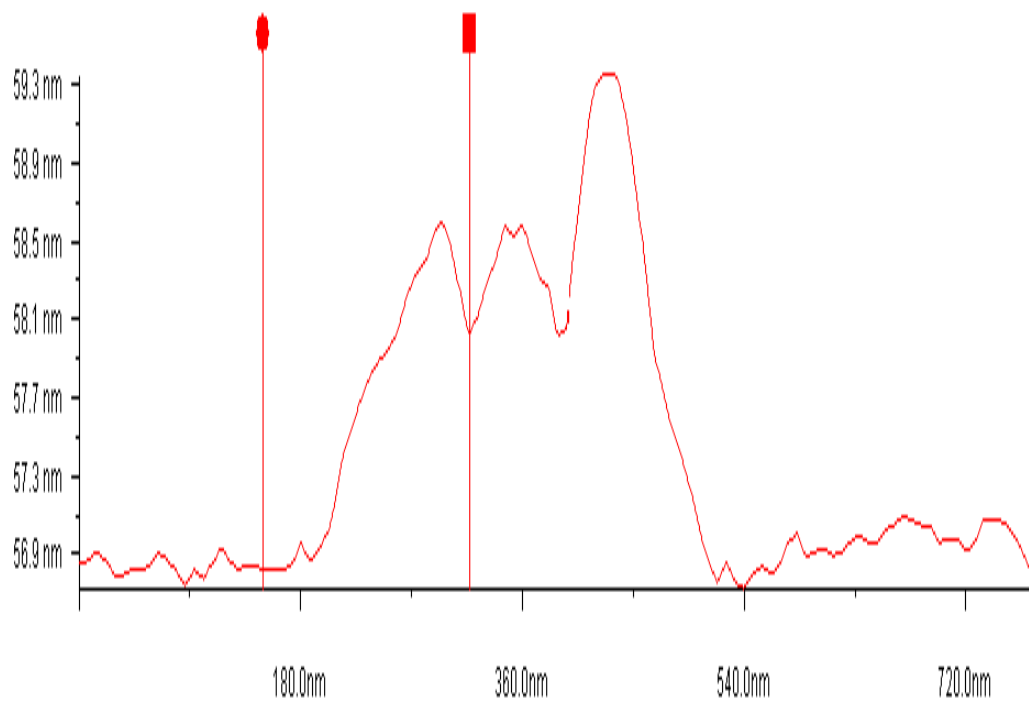
Atomic force microscopy in tapping mode was used for the investigation height profile of exfoliated graphene oxide sheet as shown in Fig.5-5. The graphene oxide height profiles typically ranged between 1 nm and 3 nm which are slightly larger than single layer graphene. The thickness of GO increased is caused by the attachment of functional groups containing oxygen, resulting GO slightly thicker, changing its surface [139].

Image(512) : Topography
3.69 x 3.69 μm x 65.3 nm





Z1		[nm]	56.7
Z2		[nm]	57.9
Z1-Z2		[nm]	1.20
Length		[um]	0.168
ANGLE		[deg]	0.407



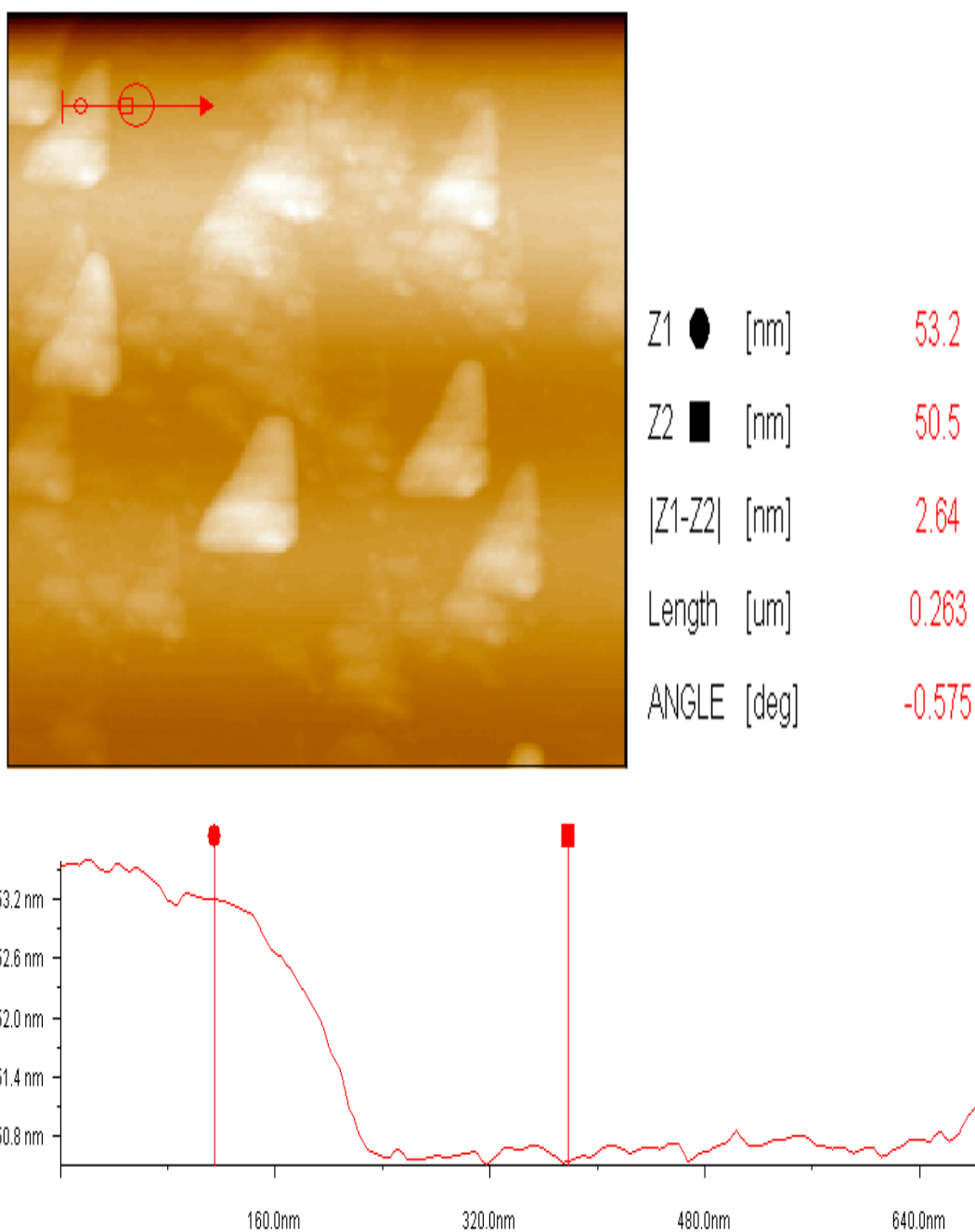


Figure 5-5: AFM Images with height profile of GO nanosheet

5.1.5 FT-IR analysis of GO and rGO

FT-IR spectra analysis was used for the purpose of investigating functional group and structure of GO sheet as seen in Fig.5-6 (a). FT-IR spectra of GO sheet indicates C=O (carboxyl), C=C(aromatic), C-O, C-H spectra and O-H(hydroxyl) groups. The presence of C-O and C=O which are the functional groups containing oxygen, further conformed the formation of GO.

Fig.5-6 (b) shows the FT-IR spectra of chemically reduced graphene oxide with the help of hydrazine hydrate indicate that much of the oxide groups (C=O) of GO are detached.

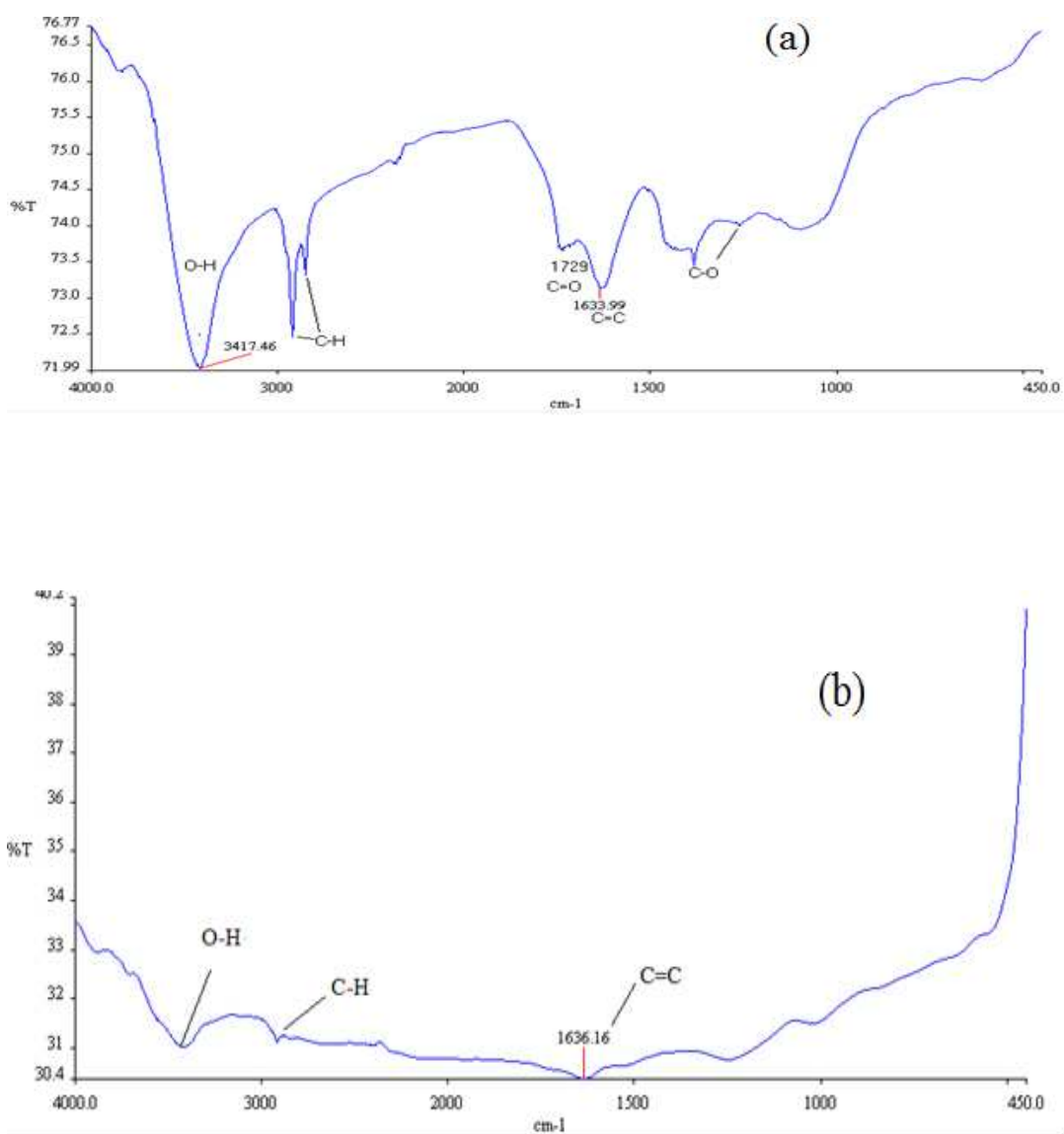


Figure 5-6: FT-IR spectra of (a) GO and (b) rGO

5.2 Characterization of Tin oxide and Graphene (rGO)/Tin oxide Composite

5.2.1 X-Ray Diffraction (XRD)

The pure SnO powder and rGO/SnO composite crystalline structure were characterized with the help of X-Ray Diffraction. The Fig.5-7 comprises the diffraction peaks of pure SnO powder and various samples of resultant Graphene/SnO composite synthesized by changing GO concentration to SnCl₂ (1.1 mmol/1-3 mg) in precursor solution of hydrothermal process. The tetragonal SnO structure crystallized completely is clearly evidenced by diffraction peaks at $2\theta=29.8$ (101), 33.2(110), 37.1(002), 47.7(200), 51.6(201), 57.3(211), 62.5(103) (JCPDS 01-072-1012).

By adding graphene oxide with different concentration to SnCl₂ developing rGO/SnO composite, there is a very small change by small wide peaks indicated at $2\theta=26^\circ$ described as a graphene peak. Graphene showing a very small peak probably because of using a very small quantity, self-reassembling of GO or reduction of GO through hydrothermal technique [140, 141]. In Graphene/SnO composite, decreasing the ratio of GO to SnCl₂ results in weakening of (002) peak and strengthening of (110) peak. The crystallite size measured through Scherrer equation, ranging from 25 nm to 53 nm.

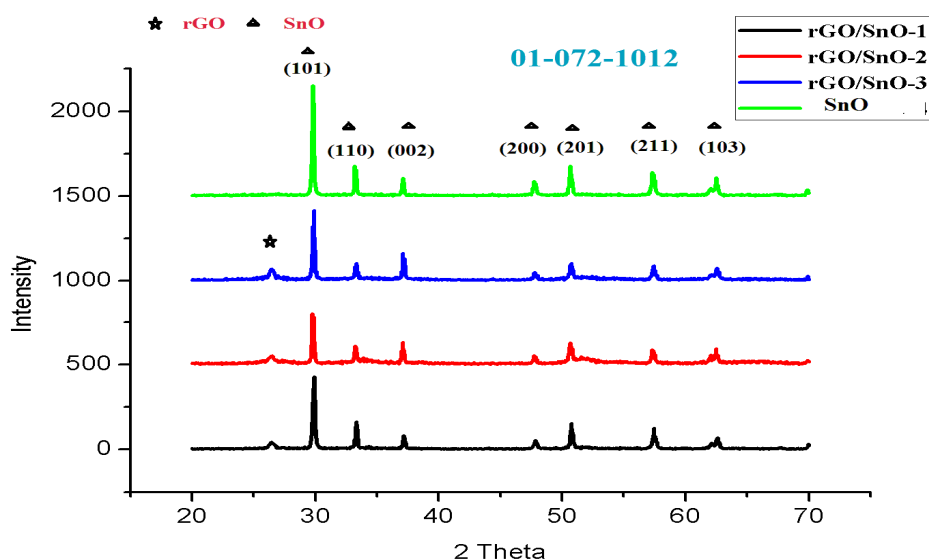


Figure 5-7: XRD Patterns of SnO and rGO /SnO composite samples

5.2.2 Scanning Electron Microscope (SEM):

The sample of SnO and rGO/SnO were prepared as a drop on silica substrate .Fig.5-8 shows the image of SnO powder indicating presence of agglomeration.

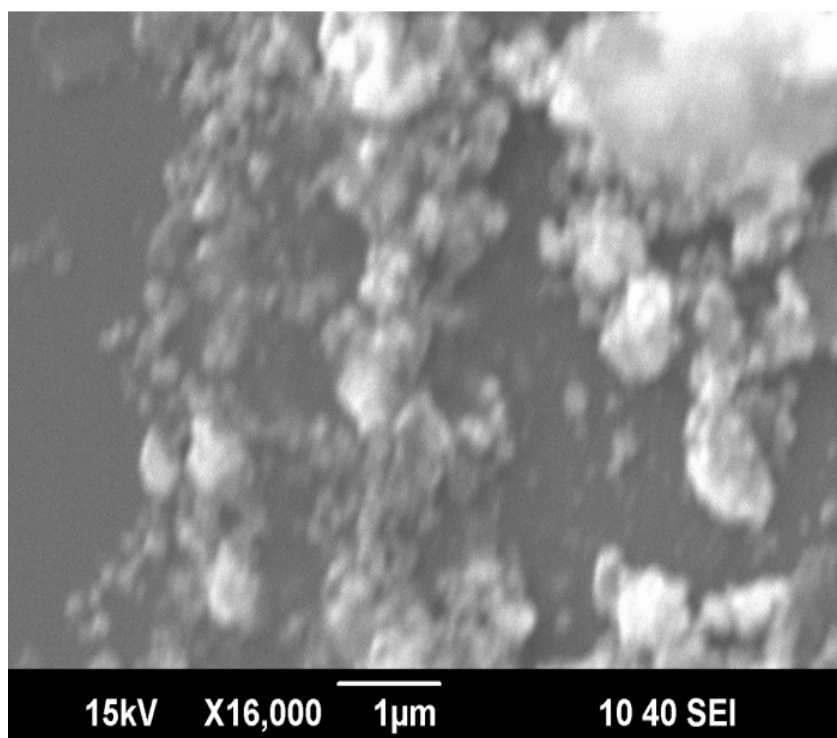


Figure 5-8: SEM image of SnO particle

rGO/SnO composite SEM images are shown in Fig.5-9 prepared through hydrothermal process. The composite are not homogeneous, there are SnO aggregates, many SnO nanoparticles covering on the surface of graphene and also some SnO nanoparticles laying in background are also observed. SEM images indicates that graphene maintain its basic structure after hydrothermal process.

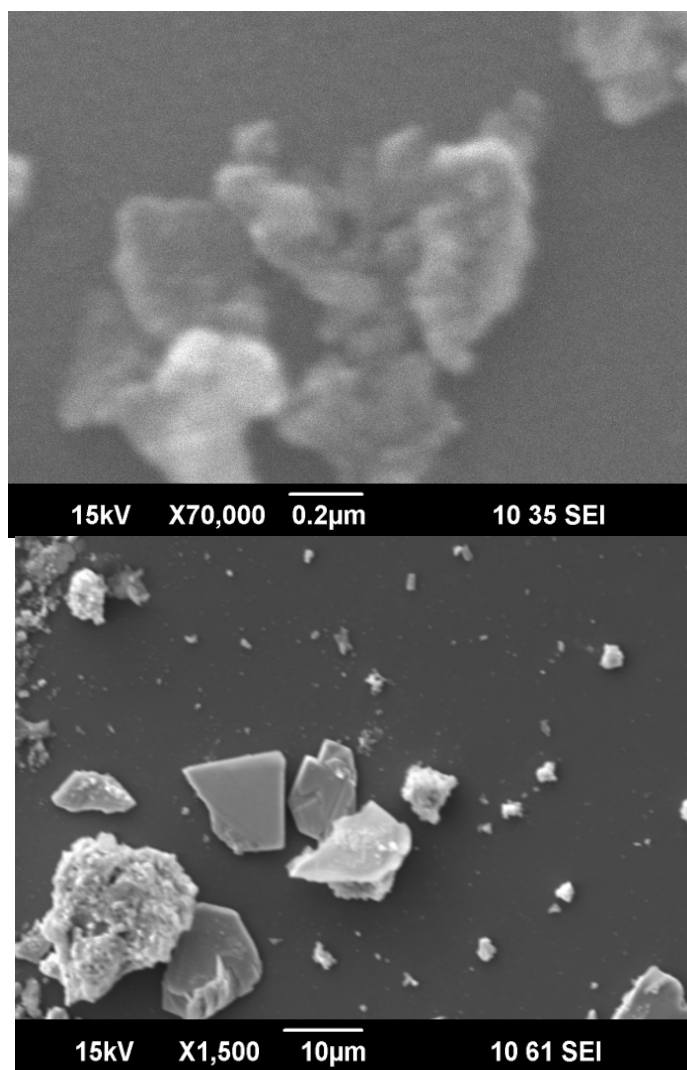


Figure 5-9: SEM images of rGO/SnO composite

5.2.3 Energy Dispersive Spectroscopy (EDS) of rGO/SnO Composite

The elemental composition of resultant rGO/SnO composite was confirmed by EDS analysis. The EDS analysis spectrum, green color peak in spectrum represents the presence of 16.98% C, 69.96% O and 13.06% Sn. The red color peaks in spectrum are those generated from substrate.

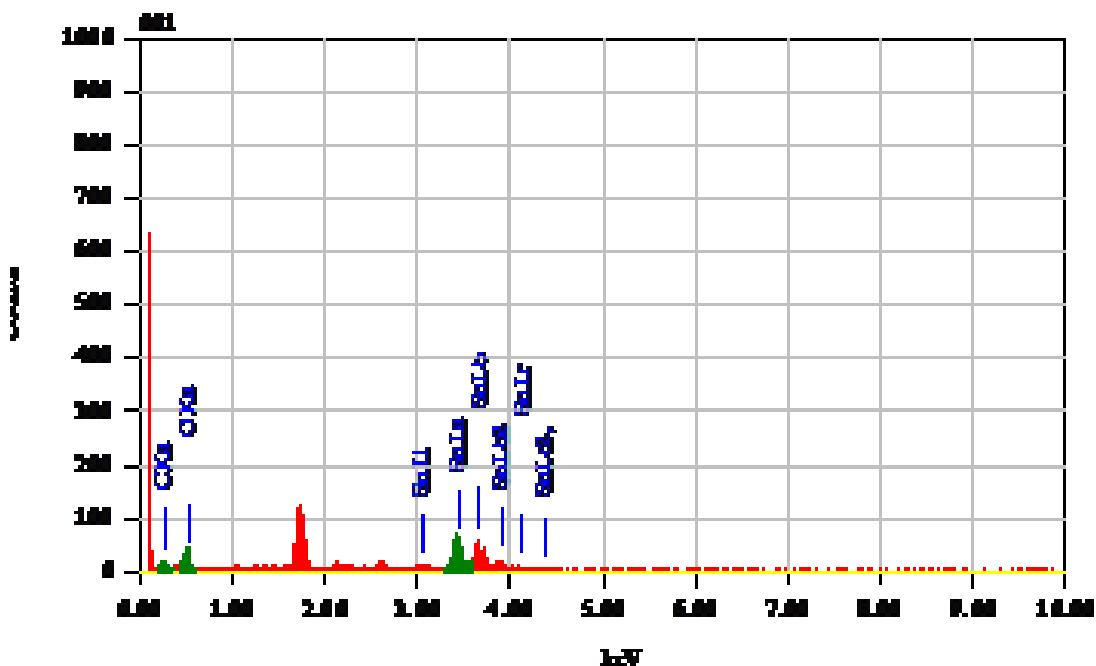


Figure 5-10: EDS spectra of rGO/SnO Composite (Green peaks: C, O, Sn)

Precursor Solution: SnCl₂/GO (1.1 mmol/3 mg)

Table 5-2: EDS Result of rGO/SnO Composite

Element	(KeV)	Mass%	Atom%
C K	0.277	7.10	16.98
O K	0.525	38.96	69.96
Sn L*	3.442	53.94	13.06
Total		100	100

5.2.4 FT-IR of rGO/SnO Composite

The Fig.5-11 shows the FT-IR spectrum of rGO/SnO composite sample. The rGO/SnO spectrum shows at $\sim 3400\text{ cm}^{-1}$ their absorption band because of O-H vibration of water molecules absorbed.

In case of GO, spectrum showing carboxyl group peak at 1729 cm^{-1} disappeared in SnO/rGO spectrum, however composite spectrum showing two strong peaks, one at

619 cm^{-1} attributes to anti-symmetric vibration Sn-O-Sn and second peak at 1629 cm^{-1} (C=C) indicate the formation of graphene network [80, 142].

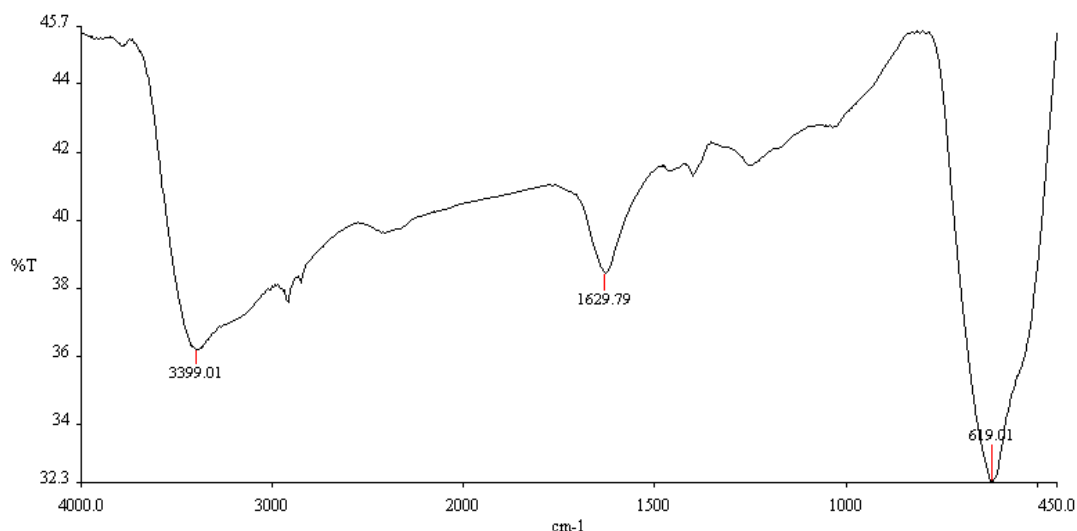


Figure 5-11: FT-IR of rGO/SnO Composite

5.3 Electrical properties of Graphene and *rGO/SnO* composite

In order to find out the electrical properties of synthesized graphene and rGO/SnO composite, the material was deposited by painting using soft brush on pre-deposited gold interdigitated electrode in such a way that bridge up these electrodes. Two probe method with the electrical instrument of Keithly source meter (2400-C) and Agilent (34401A) digital multimeter were used for the determination of current-voltage characteristic of graphene and rGO/SnO composite.

Fig.5-12 (a) shows the I-V characteristic with black line of rGO and red line of rGO/SnO-3 composite. The data represent dramatically change in I-V curve of graphene when SnO incorporated in graphene. The current drawn through the composite film decrease from mA to μA . Fig.5-12(b) shows the I-V curve of rGO/SnO composite prepared with different concentration of GO to SnCl_2 (precursor solution: $\text{SnCl}_2/\text{GO} = 1.1 \text{ mmole}/1 \text{ mg}, 1.1 \text{ mmol}/2\text{mg}, 1.1 \text{ mmol}/3 \text{ mg}$) in hydrothermal process at room temperature. The result indicates that increasing the ratio of graphene increase the conductivity of composite film. The I-V curve of fabricated rGO and rGO/SnO composite shows ohmic behavior.

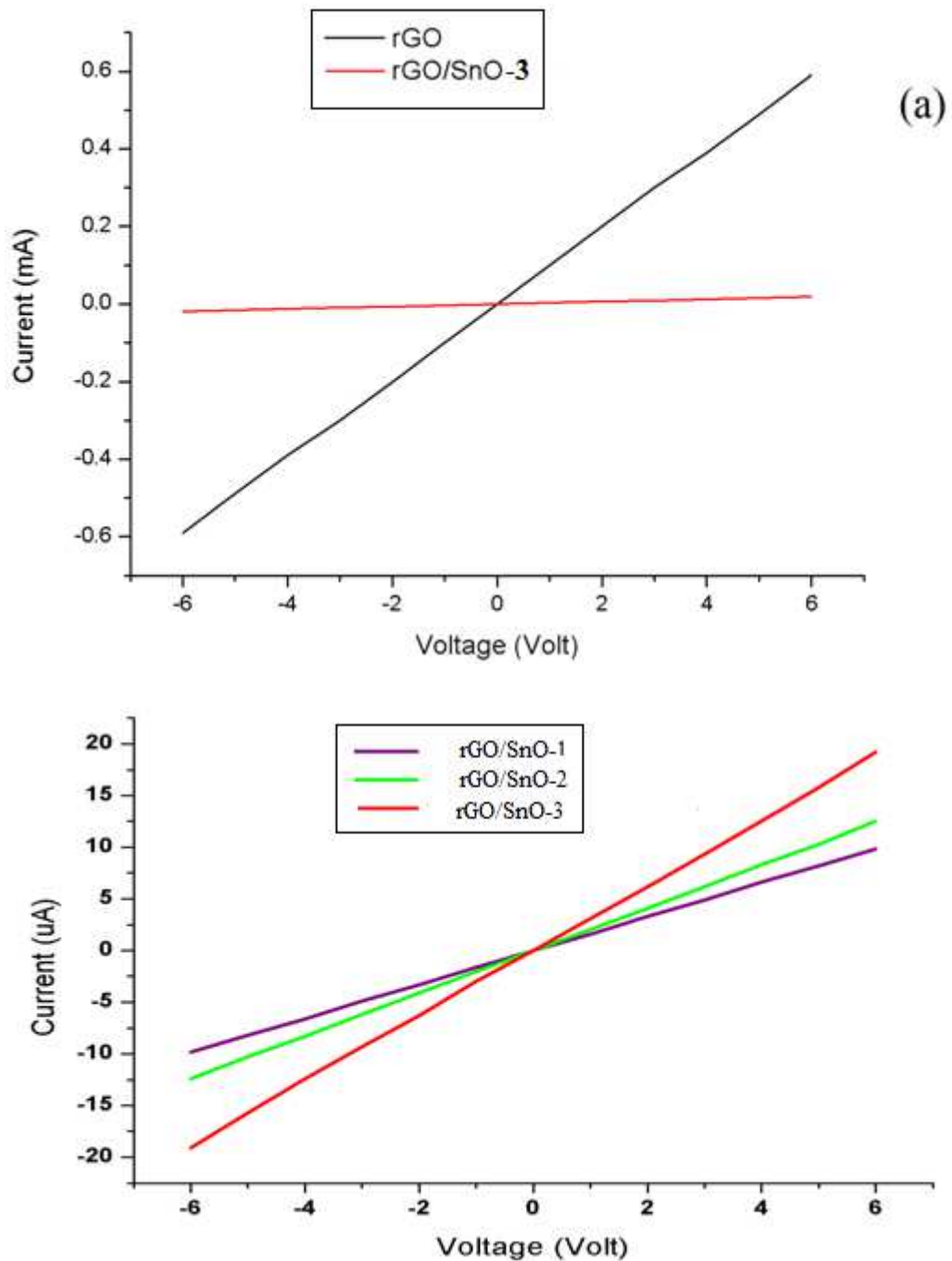


Figure 5-12: I-V characteristic of (a) rGO (b) rGO/SnO composite

The GO/SnO-3 ($\text{SnCl}_2/\text{GO} = 1.1\text{mmole}/3\text{ mg}$) composite film was allowed to test their resistance variation at different temperatures. We applied different temperature from $25\text{ }^\circ\text{C}$ to $200\text{ }^\circ\text{C}$. Fig.5-13 represents decrease in resistance from $310\text{ k}\Omega$ to $297\text{ k}\Omega$) of rGO/SnO composite film on temperature increase from $25\text{ }^\circ\text{C}$ to $200\text{ }^\circ\text{C}$ showing semiconductor behavior.

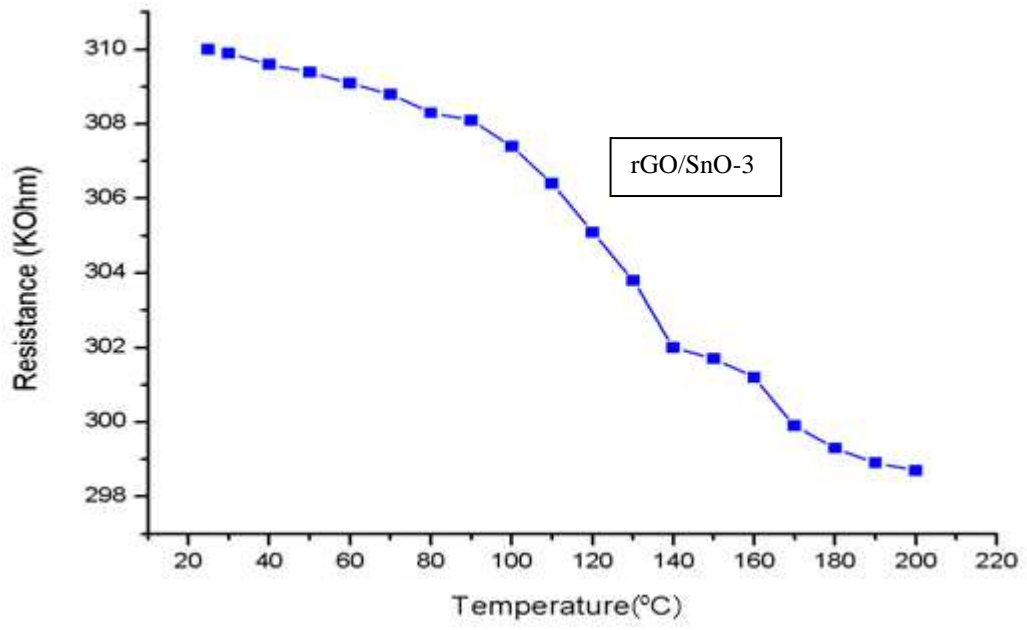


Figure 5-13: Temperature effect on rGO/SnO Composite

6. Conclusion

Graphene oxide (GO) successfully synthesized with the help of “Improved method” showing its diffraction peak at $2\theta=10.4^\circ$ with no peak at 26.4° . The graphene oxide height profiles determined by AFM in tapping mode were typically ranged between 1 nm and 3 nm.

The tetragonal SnO crystalline structure with average crystallite size of 25-53 nm synthesized, evident by XRD peaks. SEM conformed the dispersion of SnO nanoparticles on graphene sheet.

Study of I-V characteristic of graphene and rGO/SnO nanocomposite shows ohmic behavior. Significant change in the I-V characteristic of bare graphene observed on adding SnO nanoparticles, current drops from mA to μA . The nanocomposite conductivity increase with increasing graphene concentration to SnO. Resistance of rGO/SnO composite decrease from 310 K Ω to 297 K Ω with increase in temperature from 25 C⁰ to 200 C⁰, showing semiconductor behavior.

REFERENCES

- [1] C. Lok, "Small wonders," *Nature*, vol. 467, pp. 18-19, 2010.
- [2] K. Chattopadhyay, *Introduction To Nanoscience And Nanotechnology*: PHI Learning Pvt. Ltd., 2009.
- [3] M. E. Davis, J. E. Zuckerman, C. H. J. Choi, D. Seligson, A. Tolcher, C. A. Alabi, *et al.*, "Evidence of RNAi in humans from systemically administered siRNA via targeted nanoparticles," *Nature*, vol. 464, pp. 1067-1070, 2010.
- [4] L. Kalaugher, "Nanotube bike enters Tour de France," *Nanotechweb.org*, 2005.
- [5] A. Eitan, K. Jiang, D. Dukes, R. Andrews, and L. S. Schadler, "Surface modification of multiwalled carbon nanotubes: toward the tailoring of the interface in polymer composites," *Chemistry of Materials*, vol. 15, pp. 3198-3201, 2003.
- [6] L. Pauling, *The nature of the chemical bond and the structure of molecules and crystals: an introduction to modern structural chemistry* vol. 18: Cornell University Press, 1960.
- [7] K. S. Novoselov, A. K. Geim, S. Morozov, D. Jiang, Y. Zhang, S. Dubonos, *et al.*, "Electric field effect in atomically thin carbon films," *science*, vol. 306, pp. 666-669, 2004.
- [8] X. Zhou, X. Huang, X. Qi, S. Wu, C. Xue, F. Y. Boey, *et al.*, "In situ synthesis of metal nanoparticles on single-layer graphene oxide and reduced graphene oxide surfaces," *The Journal of Physical Chemistry C*, vol. 113, pp. 10842-10846, 2009.
- [9] J. Du, X. Lai, N. Yang, J. Zhai, D. Kisailus, F. Su, *et al.*, "Hierarchically ordered macro-mesoporous TiO₂- graphene composite films: Improved mass transfer, reduced charge recombination, and their enhanced photocatalytic activities," *ACS nano*, vol. 5, pp. 590-596, 2010.
- [10] L.-S. Zhang, L.-Y. Jiang, H.-J. Yan, W. D. Wang, W. Wang, W.-G. Song, *et al.*, "Mono dispersed SnO₂ nanoparticles on both sides of single layer graphene sheets as anode materials in Li-ion batteries," *Journal of Materials Chemistry*, vol. 20, pp. 5462-5467, 2010.
- [11] J. Yan, T. Wei, W. Qiao, B. Shao, Q. Zhao, L. Zhang, *et al.*, "Rapid microwave-assisted synthesis of graphene nanosheet/Co₃O₄ composite for supercapacitors," *Electrochimica Acta*, vol. 55, pp. 6973-6978, 2010.
- [12] Y. Mai, X. Wang, J. Xiang, Y. Qiao, D. Zhang, C. Gu, *et al.*, "CuO/graphene composite as anode materials for lithium-ion batteries," *Electrochimica Acta*, vol. 56, pp. 2306-2311, 2011.
- [13] Z. Yin, S. Wu, X. Zhou, X. Huang, Q. Zhang, F. Boey, *et al.*, "Electrochemical deposition of ZnO nanorods on transparent reduced graphene oxide electrodes for hybrid solar cells," *Small*, vol. 6, pp. 307-312, 2010.
- [14] R. F. Curl, "Dawn of the fullerenes: experiment and conjecture," *Reviews of modern physics*, vol. 69, pp. 691-702, 1997.
- [15] S. Iijima, "Helical microtubules of graphitic carbon," *nature*, vol. 354, pp. 56-58, 1991.
- [16] K. Novoselov, A. K. Geim, S. Morozov, D. Jiang, M. K. I. Grigorieva, S. Dubonos, *et al.*, "Two-dimensional gas of massless Dirac fermions in graphene," *nature*, vol. 438, pp. 197-200, 2005.
- [17] A. K. Geim and K. S. Novoselov, "The rise of graphene," *Nature materials*, vol. 6, pp. 183-191, 2007.
- [18] B. T. Kelly, "Physics of graphite," 1981.
- [19] C. Lee, X. Wei, J. W. Kysar, and J. Hone, "Measurement of the elastic properties and intrinsic strength of monolayer graphene," *science*, vol. 321, pp. 385-388, 2008.

- [20] A. C. Ferrari, F. Bonaccorso, V. Fal'Ko, K. S. Novoselov, S. Roche, P. Bøggild, *et al.*, "Science and technology roadmap for graphene, related two-dimensional crystals, and hybrid systems," *Nanoscale*, vol. 7, pp. 4598-4810, 2015.
- [21] D. R. Dreyer, S. Murali, Y. Zhu, R. S. Ruoff, and C. W. Bielawski, "Reduction of graphite oxide using alcohols," *Journal of Materials Chemistry*, vol. 21, pp. 3443-3447, 2011.
- [22] K. Zhou, Y. Zhu, X. Yang, and C. Li, "One-pot preparation of graphene/Fe₃O₄ composites by a solvothermal reaction," *New Journal of Chemistry*, vol. 34, pp. 2950-2955, 2010.
- [23] S. Stankovich, D. A. Dikin, R. D. Piner, K. A. Kohlhaas, A. Kleinhammes, Y. Jia, *et al.*, "Synthesis of graphene-based nanosheets via chemical reduction of exfoliated graphite oxide," *Carbon*, vol. 45, pp. 1558-1565, 2007.
- [24] Y. Si and E. T. Samulski, "Exfoliated graphene separated by platinum nanoparticles," *Chemistry of Materials*, vol. 20, pp. 6792-6797, 2008.
- [25] Z. Chen, S. Berciaud, C. Nuckolls, T. F. Heinz, and L. E. Brus, "Energy transfer from individual semiconductor nanocrystals to graphene," *ACS nano*, vol. 4, pp. 2964-2968, 2010.
- [26] C. Rao, A. Sood, R. Voggu, and K. Subrahmanyam, "Some novel attributes of graphene," *The Journal of Physical Chemistry Letters*, vol. 1, pp. 572-580, 2010.
- [27] S. Guo and S. Dong, "Graphene nanosheet: synthesis, molecular engineering, thin film, hybrids, and energy and analytical applications," *Chemical Society Reviews*, vol. 40, pp. 2644-2672, 2011.
- [28] V. C. Tung, L.-M. Chen, M. J. Allen, J. K. Wassei, K. Nelson, R. B. Kaner, *et al.*, "Low-temperature solution processing of graphene-carbon nanotube hybrid materials for high-performance transparent conductors," *Nano Letters*, vol. 9, pp. 1949-1955, 2009.
- [29] F. Hao, D. Fang, and Z. Xu, "Mechanical and thermal transport properties of graphene with defects," *Applied Physics Letters*, vol. 99, p. 041901, 2011.
- [30] I. Meric, M. Y. Han, A. F. Young, B. Ozyilmaz, P. Kim, and K. L. Shepard, "Current saturation in zero-bandgap, top-gated graphene field-effect transistors," *Nature nanotechnology*, vol. 3, pp. 654-659, 2008.
- [31] O. V. Yazyev and M. Katsnelson, "Magnetic correlations at graphene edges: basis for novel spintronics devices," *Physical Review Letters*, vol. 100, p. 047209, 2008.
- [32] K. S. Kim, Y. Zhao, H. Jang, S. Y. Lee, J. M. Kim, K. S. Kim, *et al.*, "Large-scale pattern growth of graphene films for stretchable transparent electrodes," *Nature*, vol. 457, pp. 706-710, 2009.
- [33] M. Pumera, "Electrochemistry of graphene: new horizons for sensing and energy storage," *The Chemical Record*, vol. 9, pp. 211-223, 2009.
- [34] I. V. Lightcap, T. H. Kosel, and P. V. Kamat, "Anchoring semiconductor and metal nanoparticles on a two-dimensional catalyst mat. storing and shuttling electrons with reduced graphene oxide," *Nano letters*, vol. 10, pp. 577-583, 2010.
- [35] S. Stankovich, D. A. Dikin, G. H. Dommett, K. M. Kohlhaas, E. J. Zimney, E. A. Stach, *et al.*, "Graphene-based composite materials," *Nature*, vol. 442, pp. 282-286, 2006.
- [36] X. Wan, Y. Huang, and Y. Chen, "Focusing on energy and optoelectronic applications: a journey for graphene and graphene oxide at large scale," *Accounts of chemical research*, vol. 45, pp. 598-607, 2012.
- [37] S. Stankovich, R. D. Piner, S. T. Nguyen, and R. S. Ruoff, "Synthesis and exfoliation of isocyanate-treated graphene oxide nanoplatelets," *Carbon*, vol. 44, pp. 3342-3347, 2006.
- [38] B. C. Brodie, "On the atomic weight of graphite," *Philosophical Transactions of the Royal Society of London*, pp. 249-259, 1859.

- [39] L. Staudenmaier, "Ber Dtsch Chem Ges 1898, 31, 1481–1487," *Direct Link: Abstract PDF (393K) References*.
- [40] W. S. Hummers Jr and R. E. Offeman, "Preparation of graphitic oxide," *Journal of the American Chemical Society*, vol. 80, pp. 1339-1339, 1958.
- [41] D. C. Marcano, D. V. Kosynkin, J. M. Berlin, A. Sinitskii, Z. Sun, A. Slesarev, *et al.*, "Improved synthesis of graphene oxide," *ACS nano*, vol. 4, pp. 4806-4814, 2010.
- [42] C. Zhu, S. Guo, Y. Fang, and S. Dong, "Reducing sugar: new functional molecules for the green synthesis of graphene nanosheets," *ACS nano*, vol. 4, pp. 2429-2437, 2010.
- [43] K. A. Mkhoyan, A. W. Contryman, J. Silcox, D. A. Stewart, G. Eda, C. Mattevi, *et al.*, "Atomic and electronic structure of graphene-oxide," *Nano letters*, vol. 9, pp. 1058-1063, 2009.
- [44] X. Wang, L. Zhi, and K. Müllen, "Transparent, conductive graphene electrodes for dye-sensitized solar cells," *Nano letters*, vol. 8, pp. 323-327, 2008.
- [45] G. Eda and M. Chhowalla, "Graphene-based composite thin films for electronics," *Nano Letters*, vol. 9, pp. 814-818, 2009.
- [46] N. Mohanty and V. Berry, "Graphene-based single-bacterium resolution biodevice and DNA transistor: interfacing graphene derivatives with nanoscale and microscale biocomponents," *Nano Letters*, vol. 8, pp. 4469-4476, 2008.
- [47] J. Liang, Y. Xu, D. Sui, L. Zhang, Y. Huang, Y. Ma, *et al.*, "Flexible, magnetic, and electrically conductive graphene/Fe₃O₄ paper and its application for magnetic-controlled switches," *The Journal of Physical Chemistry C*, vol. 114, pp. 17465-17471, 2010.
- [48] D. A. Dikin, S. Stankovich, E. J. Zimney, R. D. Piner, G. H. Dommett, G. Evmenenko, *et al.*, "Preparation and characterization of graphene oxide paper," *Nature*, vol. 448, pp. 457-460, 2007.
- [49] J. S. Bunch, A. M. Van Der Zande, S. S. Verbridge, I. W. Frank, D. M. Tanenbaum, J. M. Parpia, *et al.*, "Electromechanical resonators from graphene sheets," *Science*, vol. 315, pp. 490-493, 2007.
- [50] R. W. G. Wyckoff, *Crystal structures*: Krieger, 1964.
- [51] M. Fernández-García and J. A. Rodríguez, "Metal oxide nanoparticles," *Encyclopedia of Inorganic and Bioinorganic Chemistry*, 2007.
- [52] P. Ayyub, V. Palkar, S. Chattopadhyay, and M. Multani, "Effect of crystal size reduction on lattice symmetry and cooperative properties," *Physical Review B*, vol. 51, p. 6135, 1995.
- [53] P. Moriarty, "Nanostructured materials," *Reports on Progress in Physics*, vol. 64, p. 297, 2001.
- [54] J. A. Rodríguez, "Orbital-band interactions and the reactivity of molecules on oxide surfaces: from explanations to predictions," *Theoretical Chemistry Accounts*, vol. 107, pp. 117-129, 2002.
- [55] M. Fernández-García, J. C. Conesa, and F. Illas, "Effect of the Madelung potential value and symmetry on the adsorption properties of adsorbate/oxide systems," *Surface science*, vol. 349, pp. 207-215, 1996.
- [56] T. Albright, J. Burdett, and M. Whangbo, "Orbital Interactions in Chemistry" Wiley-Interscience, New York, 1985.
- [57] D.-W. Yuan, R.-F. Yan, and G. Simkovich, "Rapid oxidation of liquid tin and its alloys at 600 to 800 C," *Journal of materials science*, vol. 34, pp. 2911-2920, 1999.
- [58] R. Hart, "The thermal oxidation of tin," *Proceedings of the Physical Society. Section B*, vol. 65, p. 955, 1952.
- [59] S. M. Ali, J. Muhammad, S. T. Hussain, S. A. Bakar, and M. Ashraf, "Study of microstructural, optical and electrical properties of Mg doped SnO thin films," *Journal of Materials Science: Materials in Electronics*, vol. 24, pp. 2432-2437, 2013.

- [60] H. Giefers, F. Porsch, and G. Wortmann, "Kinetics of the disproportionation of SnO," *Solid State Ionics*, vol. 176, pp. 199-207, 2005.
- [61] S. Das, S. Chaudhuri, and S. Maji, "Ethanol-water mediated solvothermal synthesis of cube and pyramid shaped nanostructured tin oxide," *The Journal of Physical Chemistry C*, vol. 112, pp. 6213-6219, 2008.
- [62] P. Pandey, B. Upadhyay, C. Pandey, and H. Pathak, "Electrochemical studies on D96N bacteriorhodopsin and its application in the development of photosensors," *Sensors and Actuators B: Chemical*, vol. 56, pp. 112-120, 1999.
- [63] Z. Hong, C. Liang, X. Sun, and X. Zeng, "Characterization of organic photovoltaic devices with indium-tin-oxide anode treated by plasma in various gases," *Journal of applied physics*, vol. 100, p. 093711, 2006.
- [64] C. Branci, N. Benjelloun, J. Sarradin, and M. Ribes, "Vitreous tin oxide-based thin film electrodes for Li-ion micro-batteries," *Solid State Ionics*, vol. 135, pp. 169-174, 2000.
- [65] J. Calderer, P. Molinas, J. Sueiras, E. Llobet, X. Vilanova, X. Correig, *et al.*, "Synthesis and characterisation of metal suboxides for gas sensors," *Microelectronics Reliability*, vol. 40, pp. 807-810, 2000.
- [66] M. Batzill and U. Diebold, "The surface and materials science of tin oxide," *Progress in surface science*, vol. 79, pp. 47-154, 2005.
- [67] M. Meyer, G. Onida, A. Ponchel, and L. Reining, "Electronic structure of stannous oxide," *Computational materials science*, vol. 10, pp. 319-324, 1998.
- [68] Y. Xue, H. Chen, D. Yu, S. Wang, M. Yardeni, Q. Dai, *et al.*, "Oxidizing metal ions with graphene oxide: the in situ formation of magnetic nanoparticles on self-reduced graphene sheets for multifunctional applications," *Chemical Communications*, vol. 47, pp. 11689-11691, 2011.
- [69] P. Teo, H. Lim, N. Huang, C. Chia, and I. Harrison, "Room temperature in situ chemical synthesis of Fe₃O₄/graphene," *Ceramics International*, vol. 38, pp. 6411-6416, 2012.
- [70] Q.-h. Hu, X.-t. Wang, C. Hao, and Z.-f. Wang, "Synthesis of Ni/graphene sheets by an electroless Ni-plating method," *New Carbon Materials*, vol. 27, pp. 35-41, 2012.
- [71] V. Singh, D. Joung, L. Zhai, S. Das, S. I. Khondaker, and S. Seal, "Graphene based materials: past, present and future," *Progress in Materials Science*, vol. 56, pp. 1178-1271, 2011.
- [72] X. Wang, H. Tian, Y. Yang, H. Wang, S. Wang, W. Zheng, *et al.*, "Reduced graphene oxide/CdS for efficiently photocatalytic degradation of methylene blue," *Journal of Alloys and Compounds*, vol. 524, pp. 5-12, 2012.
- [73] P. Lian, X. Zhu, H. Xiang, Z. Li, W. Yang, and H. Wang, "Enhanced cycling performance of Fe₃O₄-graphene nanocomposite as an anode material for lithium-ion batteries," *Electrochimica Acta*, vol. 56, pp. 834-840, 2010.
- [74] B. Wang, J. Park, C. Wang, H. Ahn, and G. Wang, "Mn₃O₄ nanoparticles embedded into graphene nanosheets: preparation, characterization, and electrochemical properties for supercapacitors," *Electrochimica Acta*, vol. 55, pp. 6812-6817, 2010.
- [75] H. N. Lim, R. Nurzulaikha, I. Harrison, S. Lim, W. Tan, M. Yeo, *et al.*, "Preparation and characterization of tin oxide, SnO₂ nanoparticles decorated graphene," *Ceramics International*, vol. 38, pp. 4209-4216, 2012.
- [76] J. Guo, S. Zhu, Z. Chen, Y. Li, Z. Yu, Q. Liu, *et al.*, "Sonochemical synthesis of TiO₂ nanoparticles on graphene for use as photocatalyst," *Ultrasonics sonochemistry*, vol. 18, pp. 1082-1090, 2011.
- [77] A. Marlinda, N. M. Huang, M. R. Muhamad, M. An'amt, B. Y. S. Chang, N. Yusoff, *et al.*, "Highly efficient preparation of ZnO nanorods decorated reduced graphene oxide nanocomposites," *Materials Letters*, vol. 80, pp. 9-12, 2012.

- [78] C. Zhong, J. Wang, Z. Chen, and H. Liu, "SnO₂-graphene composite synthesized via an ultrafast and environmentally friendly microwave autoclave method and its use as a superior anode for lithium-ion batteries," *The Journal of Physical Chemistry C*, vol. 115, pp. 25115-25120, 2011.
- [79] S. Chen, J. Zhu, and X. Wang, "An in situ oxidation route to fabricate graphene nanoplate-metal oxide composites," *Journal of Solid State Chemistry*, vol. 184, pp. 1393-1399, 2011.
- [80] H. Seema, K. C. Kemp, V. Chandra, and K. S. Kim, "Graphene-SnO₂ composites for highly efficient photocatalytic degradation of methylene blue under sunlight," *Nanotechnology*, vol. 23, p. 355705, 2012.
- [81] C. Wu, Y. Zhang, S. Li, H. Zheng, H. Wang, J. Liu, *et al.*, "Synthesis and photocatalytic properties of the graphene-La₂Ti₂O₇ nanocomposites," *Chemical Engineering Journal*, vol. 178, pp. 468-474, 2011.
- [82] S. Moussa, V. Abdelsayed, and M. S. El-Shall, "Laser synthesis of Pt, Pd, CoO and Pd-CoO nanoparticle catalysts supported on graphene," *Chemical Physics Letters*, vol. 510, pp. 179-184, 2011.
- [83] Y. Wei, C. Gao, F.-L. Meng, H.-H. Li, L. Wang, J.-H. Liu, *et al.*, "SnO₂/reduced graphene oxide nanocomposite for the simultaneous electrochemical detection of cadmium (II), lead (II), copper (II), and mercury (II): an interesting favorable mutual interference," *The Journal of Physical Chemistry C*, vol. 116, pp. 1034-1041, 2011.
- [84] J. Yao, X. Shen, B. Wang, H. Liu, and G. Wang, "In situ chemical synthesis of SnO₂-graphene nanocomposite as anode materials for lithium-ion batteries," *Electrochemistry Communications*, vol. 11, pp. 1849-1852, 2009.
- [85] B. Su, D. Tang, Q. Li, J. Tang, and G. Chen, "Gold-silver-graphene hybrid nanosheets-based sensors for sensitive amperometric immunoassay of alpha-fetoprotein using nanogold-enclosed titania nanoparticles as labels," *Analytica chimica acta*, vol. 692, pp. 116-124, 2011.
- [86] J. Zhu, S. Wei, H. Gu, S. B. Rapole, Q. Wang, Z. Luo, *et al.*, "One-pot synthesis of magnetic graphene nanocomposites decorated with core@ double-shell nanoparticles for fast chromium removal," *Environmental science & technology*, vol. 46, pp. 977-985, 2011.
- [87] Y. Wang and J. Y. Lee, "Microwave-assisted synthesis of SnO₂-graphite nanocomposites for Li-ion battery applications," *Journal of power sources*, vol. 144, pp. 220-225, 2005.
- [88] V. Subramanian, W. W. Burke, H. Zhu, and B. Wei, "Novel microwave synthesis of nanocrystalline SnO₂ and its electrochemical properties," *The Journal of Physical Chemistry C*, vol. 112, pp. 4550-4556, 2008.
- [89] S. Wang, S. P. Jiang, and X. Wang, "Microwave-assisted one-pot synthesis of metal/metal oxide nanoparticles on graphene and their electrochemical applications," *Electrochimica Acta*, vol. 56, pp. 3338-3344, 2011.
- [90] S. Zakarya, A. Kassim, H. Lim, N. Anwar, and N. Huang, "Synthesis of titanium dioxide microstructures via sucrose ester microemulsion-mediated hydrothermal method," *Sains Malaysiana*, vol. 39, pp. 975-979, 2010.
- [91] N. S. Anwar, A. Kassim, H. N. Lim, S. Zakarya, and N. M. Huang, "Synthesis of titanium dioxide nanoparticles via sucrose ester micelle-mediated hydrothermal processing route," *Sains Malaysiana*, vol. 39, pp. 261-265, 2010.
- [92] B. Y. S. Chang, N. M. Huang, M. N. An'amt, A. R. Marlinda, Y. Norazriena, M. R. Muhamad, *et al.*, "Facile hydrothermal preparation of titanium dioxide decorated reduced graphene oxide nanocomposite," *International journal of nanomedicine*, vol. 7, p. 3379, 2012.

- [93] C. Haw, F. Mohamed, C. Chia, S. Radiman, S. Zakaria, N. Huang, *et al.*, "Hydrothermal synthesis of magnetite nanoparticles as MRI contrast agents," *Ceramics International*, vol. 36, pp. 1417-1422, 2010.
- [94] J. Xie, W. Song, Y. Zheng, S. Liu, T. Zhu, G. Cao, *et al.*, "Preparation and Li-storage properties of SnSb/graphene hybrid nanostructure by a facile one-step solvothermal route," *International Journal of Smart and Nano Materials*, vol. 2, pp. 261-271, 2011.
- [95] P. Lian, X. Zhu, S. Liang, Z. Li, W. Yang, and H. Wang, "High reversible capacity of SnO₂/graphene nanocomposite as an anode material for lithium-ion batteries," *Electrochimica Acta*, vol. 56, pp. 4532-4539, 2011.
- [96] J. Zhang, L.-B. Kong, B. Wang, Y.-C. Luo, and L. Kang, "In-situ electrochemical polymerization of multi-walled carbon nanotube/polyaniline composite films for electrochemical supercapacitors," *Synthetic Metals*, vol. 159, pp. 260-266, 2009.
- [97] J. Gong, X. Miao, H. Wan, and D. Song, "Facile synthesis of zirconia nanoparticles-decorated graphene hybrid nanosheets for an enzymeless methyl parathion sensor," *Sensors and Actuators B: Chemical*, vol. 162, pp. 341-347, 2012.
- [98] J. Gong, T. Zhou, D. Song, and L. Zhang, "Monodispersed Au nanoparticles decorated graphene as an enhanced sensing platform for ultrasensitive stripping voltammetric detection of mercury (II)," *Sensors and Actuators B: Chemical*, vol. 150, pp. 491-497, 2010.
- [99] A. Ballesteros-Gómez, S. Rubio, and D. Pérez-Bendito, "Analytical methods for the determination of bisphenol A in food," *Journal of Chromatography A*, vol. 1216, pp. 449-469, 2009.
- [100] H. Yin, L. Cui, Q. Chen, W. Shi, S. Ai, L. Zhu, *et al.*, "Amperometric determination of bisphenol A in milk using PAMAM-Fe₃O₄ modified glassy carbon electrode," *Food Chemistry*, vol. 125, pp. 1097-1103, 2011.
- [101] H. N. Lim, R. Nurzulaikha, I. Harrison, S. Lim, W. Tan, and M. Yeo, "Spherical tin oxide, SnO₂ particles fabricated via facile hydrothermal method for detection of mercury (II) ions," *International Journal of Electrochemical Science*, vol. 6, 2011.
- [102] B. M. Matin, Y. Mortazavi, A. A. Khodadadi, A. Abbasi, and A. A. Firooz, "Alkaline-and template-free hydrothermal synthesis of stable SnO₂ nanoparticles and nanorods for CO and ethanol gas sensing," *Sensors and Actuators B: Chemical*, vol. 151, pp. 140-145, 2010.
- [103] Q. Lin, Y. Li, and M. Yang, "Tin oxide/graphene composite fabricated via a hydrothermal method for gas sensors working at room temperature," *Sensors and Actuators B: Chemical*, vol. 173, pp. 139-147, 2012.
- [104] G. Neri, S. G. Leonardi, M. Latino, N. Donato, S. Baek, D. E. Conte, *et al.*, "Sensing behavior of SnO₂/reduced graphene oxide nanocomposites toward NO₂," *Sensors and Actuators B: Chemical*, vol. 179, pp. 61-68, 2013.
- [105] H. I. Becker, "Low voltage electrolytic capacitor," ed: Google Patents, 1957.
- [106] Q.-Y. Li, Z.-S. Li, L. Lin, X. Wang, Y.-F. Wang, C.-H. Zhang, *et al.*, "Facile synthesis of activated carbon/carbon nanotubes compound for supercapacitor application," *Chemical Engineering Journal*, vol. 156, pp. 500-504, 2010.
- [107] Z. S. Wu, D. W. Wang, W. Ren, J. Zhao, G. Zhou, F. Li, *et al.*, "Anchoring Hydrous RuO₂ on Graphene Sheets for High-Performance Electrochemical Capacitors," *Advanced Functional Materials*, vol. 20, pp. 3595-3602, 2010.
- [108] F. Li, J. Song, H. Yang, S. Gan, Q. Zhang, D. Han, *et al.*, "One-step synthesis of graphene/SnO₂ nanocomposites and its application in electrochemical supercapacitors," *Nanotechnology*, vol. 20, p. 455602, 2009.
- [109] I. R. Kottegoda, N. H. Idris, L. Lu, J.-Z. Wang, and H.-K. Liu, "Synthesis and characterization of graphene-nickel oxide nanostructures for fast charge-discharge application," *Electrochimica Acta*, vol. 56, pp. 5815-5822, 2011.

- [110] S. Chaturvedi and P. N. Dave, "Environmental Application of Photocatalysis," in *Materials Science Forum*, 2013, pp. 273-294.
- [111] Y. He, Y. Wu, H. Guo, T. Sheng, and X. Wu, "Visible light photodegradation of organics over VYO composite catalyst," *Journal of hazardous materials*, vol. 169, pp. 855-860, 2009.
- [112] H. Zhang, X. Lv, Y. Li, Y. Wang, and J. Li, "P25-graphene composite as a high performance photocatalyst," *ACS nano*, vol. 4, pp. 380-386, 2009.
- [113] M. Soltaninezhad and A. Aminifar, "Study nanostructures of semiconductor zinc oxide (ZnO) as a photocatalyst for the degradation of organic pollutants," *International Journal of Nano Dimension*, vol. 2, pp. 137-145, 2011.
- [114] K. Zhou, Y. Zhu, X. Yang, X. Jiang, and C. Li, "Preparation of graphene-TiO₂ composites with enhanced photocatalytic activity," *New Journal of Chemistry*, vol. 35, pp. 353-359, 2011.
- [115] B. Li and H. Cao, "ZnO@ graphene composite with enhanced performance for the removal of dye from water," *journal of materials chemistry*, vol. 21, pp. 3346-3349, 2011.
- [116] J. Zhang, Z. Xiong, and X. Zhao, "Graphene-metal-oxide composites for the degradation of dyes under visible light irradiation," *journal of materials chemistry*, vol. 21, pp. 3634-3640, 2011.
- [117] K. Novoselov, D. Jiang, F. Schedin, T. Booth, V. Khotkevich, S. Morozov, *et al.*, "Two-dimensional atomic crystals," *Proceedings of the National Academy of Sciences of the United States of America*, vol. 102, pp. 10451-10453, 2005.
- [118] J. Bernal, "The structure of graphite," *Proceedings of the Royal Society of London. Series A, Containing Papers of a Mathematical and Physical Character*, pp. 749-773, 1924.
- [119] A. Buchsteiner, A. Lerf, and J. Pieper, "Water dynamics in graphite oxide investigated with neutron scattering," *The Journal of Physical Chemistry B*, vol. 110, pp. 22328-22338, 2006.
- [120] S. Park and R. Ruoff, "Chemical methods for the production of graphenes. *Nature Nanotechnol*, 4, 217 (2009)," ed, 2009.
- [121] D. Li, M. B. Müller, S. Gilje, R. B. Kaner, and G. G. Wallace, "Processable aqueous dispersions of graphene nanosheets," *Nature nanotechnology*, vol. 3, pp. 101-105, 2008.
- [122] G. Williams, B. Seger, and P. V. Kamat, "TiO₂-graphene nanocomposites. UV-assisted photocatalytic reduction of graphene oxide," *ACS nano*, vol. 2, pp. 1487-1491, 2008.
- [123] J. Van De Lagemaat, T. M. Barnes, G. Rumbles, S. E. Shaheen, T. J. Coutts, C. Weeks, *et al.*, "Organic solar cells with carbon nanotubes replacing In₂O₃: Sn as the transparent electrode," *Applied Physics Letters*, vol. 88, p. 233503, 2006.
- [124] R. Muszynski, B. Seger, and P. V. Kamat, "Decorating graphene sheets with gold nanoparticles," *The Journal of Physical Chemistry C*, vol. 112, pp. 5263-5266, 2008.
- [125] C. Gómez-Navarro, R. T. Weitz, A. M. Bittner, M. Scolari, A. Mews, M. Burghard, *et al.*, "Electronic transport properties of individual chemically reduced graphene oxide sheets," *Nano letters*, vol. 7, pp. 3499-3503, 2007.
- [126] P. R. Somani, S. P. Somani, and M. Umeno, "Planer nano-graphenes from camphor by CVD," *Chemical Physics Letters*, vol. 430, pp. 56-59, 2006.
- [127] A. Obraztsov, E. Obraztsova, A. Tyurnina, and A. Zolotukhin, "Chemical vapor deposition of thin graphite films of nanometer thickness," *Carbon*, vol. 45, pp. 2017-2021, 2007.
- [128] D. V. Kosynkin, A. L. Higginbotham, A. Sinitskii, J. R. Lomeda, A. Dimiev, B. K. Price, *et al.*, "Longitudinal unzipping of carbon nanotubes to form graphene nanoribbons," *Nature*, vol. 458, pp. 872-876, 2009.

- [129] V. Barone, O. Hod, and G. E. Scuseria, "Electronic structure and stability of semiconducting graphene nanoribbons," *Nano letters*, vol. 6, pp. 2748-2754, 2006.
- [130] Y. Hernandez, V. Nicolosi, M. Lotya, F. M. Blighe, Z. Sun, S. De, *et al.*, "High-yield production of graphene by liquid-phase exfoliation of graphite," *Nature nanotechnology*, vol. 3, pp. 563-568, 2008.
- [131] M. Choucair, P. Thordarson, and J. A. Stride, "Gram-scale production of graphene based on solvothermal synthesis and sonication," *Nature Nanotechnology*, vol. 4, pp. 30-33, 2009.
- [132] V. K. Pecharsky and P. Y. Zavalij, *Fundamentals of powder diffraction and structural characterization of materials* vol. 2: Springer, 2009.
- [133] Y. Wang, *Silicon carbide nanowires and composites obtained from carbon nanotubes*: ProQuest, 2006.
- [134] M. T. Postek, K. S. Howard, A. H. Johnson, and K. L. McMichael, "Scanning Electron Microscopy: A Student's Handbook. Ladd Research Industries," *Inc, Burlington, VT*, 1980.
- [135] A. R. Clarke and C. N. Eberhardt, *Microscopy techniques for materials science*: Woodhead Publishing, 2002.
- [136] G. M. Crankovic, *ASM Handbook, Volume 10:: Materials Characterization*: ASM International, 1986.
- [137] Y. Li, L. Tang, and J. Li, "Preparation and electrochemical performance for methanol oxidation of pt/graphene nanocomposites," *Electrochemistry Communications*, vol. 11, pp. 846-849, 2009.
- [138] K. Haubner, J. Murawski, P. Olk, L. M. Eng, C. Ziegler, B. Adolphi, *et al.*, "The route to functional graphene oxide," *ChemPhysChem*, vol. 11, pp. 2131-2139, 2010.
- [139] J. Song, X. Wang, and C.-T. Chang, "Preparation and characterization of graphene oxide," *Journal of Nanomaterials*, vol. 2014, 2014.
- [140] H. Zhang, J. Feng, T. Fei, S. Liu, and T. Zhang, "SnO₂ nanoparticles-reduced graphene oxide nanocomposites for NO₂ sensing at low operating temperature," *Sensors and Actuators B: Chemical*, vol. 190, pp. 472-478, 2014.
- [141] S.-M. Paek, E. Yoo, and I. Honma, "Enhanced cyclic performance and lithium storage capacity of SnO₂/graphene nanoporous electrodes with three-dimensionally delaminated flexible structure," *Nano letters*, vol. 9, pp. 72-75, 2008.
- [142] L. Liu, M. An, P. Yang, and J. Zhang, "Superior cycle performance and high reversible capacity of SnO₂/graphene composite as an anode material for lithium-ion batteries," *Scientific reports*, vol. 5, 2015.